



Norwegian University  
of Life Sciences

Master's Thesis 2017

30 credits

Department of Mathematical Sciences and Technology

# **Effect of Cortical Feedback on Nerve-Cell Response in Lateral Geniculate Nucleus (LGN) to Visual Stimuli**

Effekt av Kortikal Tilbakesending av Signaler på  
Nervecellerespons i Lateral Geniculate Nucleus  
(LGN) ved Visuell Stimuli

Helene B. Midtfjord  
Computational neuroscience







# Acknowledgements

This thesis completes my master's degree in Technology at the Norwegian University of Life Sciences (NMBU).

I would like to thank my supervisor Professor Gaute T. Einevoll, who has introduced me to the exiting world of neuroscience, and included me in the educational and sociable consortium at CINPLA. I would also like to thank my co-supervisor, Milad Mobarhan, who provided me with reading material when I was curious, and gave me advice when I was confused. Thank you both for sharing ideas, knowledge and enthusiasm for the subject.

Also, I must thank Tor Næsje and Linda M. B. Thinn for putting their effort on the time consuming task of proofreading this thesis, and for making exceptional discussion partners. Finally, I would like to thank my family and boyfriend for their invaluable support and encouragement.

Ås, May 15th, 2017

---

Helene B. Midtfjord

# Abstract

A feedback connection from the visual cortex has been shown to affect characteristics of cells in the lateral geniculate nucleus (LGN) in the brain. Research of cortical feedback have been performed with experiments and modelling, but its functional role is still not resolved. Studies of cortical feedback on LGN cells found in literature mainly focus on the feedback's spatial effect on the LGN cell. The aim for this thesis is to study the feedback's temporal effects on LGN cells with the use of a newly developed tool: A neural circuit simulation software, pylgn. This simulation tool had not been tested prior to this thesis for scientific purposes by others than the developer himself. Thus, this study is the first application of pylgn.

Results of simulations of the relay-cell response with the use of pylgn featured effects in accordance with experimental research results found in literature, for example, suppression of LGN cell response when stimulus sizes are magnified over a certain diameter value. This thesis' study of effects from cortical feedback's temporal features was performed by simulations of a neural network with separated excitatory and inhibitory feedback components. Impact of delay and prolonging of feedback was studied for each feedback component. The results revealed dependence of the temporal oscillation of the neural response and the size of the stimulus for an oscillating spot and a patch grating of lower spatial frequency ( $k = 1, 47/\text{deg}$ ), but no corresponding dependence for stimulus of a patch grating with higher spatial frequency ( $k = 1, 47/\text{deg}$ ). The results showed that the dependence of the temporal oscillation of neural responses and the size of the stimulus occurred for delayed or prolonged excitatory feedback. A temporal shift in the response was also observed for delayed or prolonged excitatory feedback. The results also revealed that the oscillations in neural response for delayed or prolonged inhibitory feedback were less dependent of the patch size. This indicates that the effect of inhibitory feedback is simply to reduce response of LGN relay cells, while the excitatory feedback potentially determines the behaviour of the LGN relay cell response.

# Sammen drag

Det er bevist at en kobling som gjennomfører tilbakesending av signaler fra den visuelle hjernebarken (korteks) har effekt på egenskapene til nerveceller i lateral geniculate nucleus (LGN) i hjernen. Forskning på kortikal tilbakesending av signaler har blitt gjennomført med eksperimenter og modellering, men dens funksjonelle rolle er fremdeles ikke avklart. Studier av kortikal tilbakesending funnet i litteraturen fokuserer i hovedsak på tilbakesendingens romlige effekter på celler i LGN. Målet med denne avhandlingen er å utforske kortikal tilbakesendingens tidsmessige effekter på celler i LGN ved å benytte et nylig utviklet verktøy: En simuleringsprogramvare for nevralt nettverk, pylgn. Før denne masteroppgaven hadde dette simuleringsverktøyet ikke blitt testet til vitenskapelige formål av andre enn utvikleren selv. Dermed er denne studien den første til å benytte seg av pylgn.

Resultater fra simuleringer av respons hos relay celler ved bruk av pylgn viste effekter i samsvar med eksperimentelle resultater funnet i litteratur, for eksempel reduksjon i respons hos nerveceller i LGN når størrelsen på spotstimulusen forstørres over en viss diameterverdi. Denne avhandlingens studie av effekter fra tidsmessige egenskaper ved tilbakesending av signaler ble utført ved simulering av nevralt nettverk med separerte komponenter for eksitatorisk og inhibitorisk tilbakesending av signaler. Innvirkningen fra forsinkelse og forlengelse av tilbakesendte signaler ble studert for hver komponent av tilbakesendingen. Resultatet avdekket avhengighet mellom tidsmessig svingninger i den nevralt responsen og størrelse på spotstimulus for en blinkende spot og for en spot med gittermønster med lav romlig frekvens ( $k = 0,49/\text{deg}$ ), men ingen tilsvarende avhengighet for spotstimulus med høyere romlig frekvens ( $k = 1,47/\text{deg}$ ). Resultatene viste at denne avhengigheten mellom tidsmessig svingninger og størrelse på spotstimulus oppstod ved forsinkelse eller forlengelse av eksitatoriske tilbakesendte signaler. En tidsmessig forskyvning av respons ble også observert ved forsinket eller forlenget eksitatorisk tilbakesending. Resultatene avslørte også at svingninger i respons ved forsinkede eller forlengede inhibitoriske tilbakesendinger hadde en svakere avhengighet av størrelsen på spotstimulusen. Dette indikerer at den kvalitative effekten av inhibitorisk tilbakesending fra korteks kun er å redusere nevralt respons hos nerveceller i LGN, mens eksitatorisk tilbakesending potensielt avgjør oppførselen til responsen hos en nervecelle i LGN.





# Contents

<b>1</b>	<b>Introduction</b>	<b>1</b>
<b>2</b>	<b>Nerve Cells and Brain</b>	<b>3</b>
2.1	Nerve Cells . . . . .	3
2.1.1	Generation of Action Potentials . . . . .	3
2.1.2	Signal Transmission Between Nerve Cells . . . . .	5
2.2	Early Visual System . . . . .	5
2.2.1	Retina . . . . .	5
2.2.2	Lateral Geniculate Nucleus (LGN) . . . . .	7
2.2.3	Thalamic Reticular Nucleus (TRN) . . . . .	7
2.2.4	Visual Cortex . . . . .	7
2.2.5	Features of LGN . . . . .	8
2.3	Modelling Neurons and Their Network . . . . .	8
2.3.1	Challenges in Computational Neural Network Modelling . . . . .	9
2.3.2	Simplifications in Computational Neural Network Modelling . . . . .	9
<b>3</b>	<b>Receptive Fields</b>	<b>11</b>
3.1	Modelling of Spatial Receptive Fields . . . . .	11
3.2	Modelling of Temporal Receptive Fields . . . . .	15
<b>4</b>	<b>The Mathematical Model (eDoG for LGN Circuits)</b>	<b>19</b>
4.1	Impulse-Response Function . . . . .	19
4.2	Coupling Function . . . . .	20
4.3	The Geniculate Transfer Function . . . . .	21
4.4	Coupling Scheme . . . . .	21
4.5	Impulse-Response Function of LGN Relay Cells . . . . .	23
<b>5</b>	<b>Simulation</b>	<b>25</b>
5.1	Programming Tools . . . . .	25
5.1.1	Python . . . . .	25
5.1.2	Spyder . . . . .	25

---

5.1.3	Anaconda . . . . .	26
5.1.4	GitHub . . . . .	26
5.2	Neural Circuit Simulation Tool (pylgn) . . . . .	26
5.2.1	Example Application . . . . .	27
5.2.2	Create Network . . . . .	29
5.2.3	Create Neurons . . . . .	30
5.2.4	Choice of Coupling Functions and Parameters . . . . .	31
5.2.5	Stimuli . . . . .	33
<b>6</b>	<b>Spatial Effects of Cortical Feedback on LGN Relay Cells,</b>	<b>35</b>
6.1	Previous Work Including eDoG Model and Pylgn . . . . .	37
6.2	Validation of Network . . . . .	38
<b>7</b>	<b>Temporal Effects of Cortical Feedback on LGN Relay Cells</b>	<b>41</b>
7.1	Response to Oscillating Spot . . . . .	42
7.2	LGN Rerlay cell Response to Patch Grating . . . . .	47
7.3	Significance of Results . . . . .	50
<b>A</b>	<b>Programme Code for Simulation of Response in LGN Relay Cell to Different Stimuli with Pylgn</b>	<b>55</b>
<b>B</b>	<b>Plotting Impulse-Response for Spatial Parameters</b>	<b>59</b>

# Chapter 1

## Introduction

How the human mind works is one of the big questions. Studies of the human brain are being performed in many academic disciplines, urging for an understanding of how neurons and their connections can create our perception and ideas of the world around us. Modelling of neural network combines the expertises of mathematics, biology and computer science, and is therefore a powerful tool for gaining insight in how the brain works. The human brain consists of about 100 billion nerve cells, thus modelling an entire human brain is out of question with today's technology. However, models of smaller networks provide useful knowledge of functionality of brain. The topic of this thesis is processing of visual stimulus, and so the relevant network of modelling is a simplification of the early visual system of the brain.

The early visual system includes the retina in the eyes, the visual cortex in the back of the brain, and the lateral geniculate nucleus (LGN) in-between. The LGN is the least studied component of the early visual system, and it has been assumed that the only function of the LGN is to relay sensory information to the cortex. However, research has shown contradicting results during the last two decades [17], and there has been a growing recognition that the LGN has a more significant role in the processing of visual information. A feedback connection from the visual cortex has been shown to affect characteristics of LGN relay cells [1]. Most research on the topic discuss the spatial effect of cortical feedback on LGN neurons. Little attention has been given to temporal aspects, like delay and duration of response to a stimulus. This thesis aims to elucidate effects from these temporal aspects of the cortical feedback on LGN neurons. Experimental results have shown that inhibitory feedback is delayed compared to the excitatory feedback [7]. Previously, cortical feedback has been studied as a unity. This thesis will consider cortical feedback as two separate feedback components, one excitatory and one inhibitory. The objective of this thesis is to study temporal features of the separate cortical feedback components on the relay cells in LGN; delay and prolonging are such two

features of cortical feedback. In summary, the research question of this thesis is as follows: How does temporal delay and prolonging of separate excitatory and inhibitory cortical feedback components effect the response of the LGN relay cells?

Because selectivity for stimulus size and frequency of gratings are fundamental properties of visual neurons [1], it makes sense to explore the neural response for stimuli with different grating and different sizes. The method performed to study neural response has been the implementation of a neural circuit simulation tool (pylgn) recently developed at Centre for Integrative Neuroplasticity (CINPLA) - a strategic research initiative at the faculty of mathematics and natural sciences at UiO. The mathematical model behind pylgn is the linear, mechanistic, firing-rate based eDoG model, that incorporates the influence of thalamocortical loops, in addition to the feedforward responses. This thesis presents the first application of pylgn, and the second objective of this thesis is simply to test this tool in cooperation with the creator of the software.

How pylgn is implemented in general, and how it has been used for this thesis, is explained in chapter 5. Chapter 2 establishes a general understanding of nerve cells, the early visual system of the brain, and modelling concepts in neuroscience. Then chapter 3 explains the concept of receptive fields, which is an important, analytical construction in the study of visual processing. An outline of the mathematical eDoG model is given in chapter 4. Then, a brief introduction to spatial effects of cortical feedback is given in chapter 6. The final two chapters present the results of the simulations and a discussion the impact of the findings.

# Chapter 2

## Nerve Cells and Brain

### 2.1 Nerve Cells

There are about 100 billion ( $10^{12}$ ) nerve cells in the human brain. Each nerve cell (or neuron) communicate with to up ten thousand other neurons. They are highly adapted to generate nerve impulses (i.e. brief electrical signals) in response to input. This quality is reflected by the neuron morphology. Figure 2.1 shows three examples of nerve cells: A cortical pyramidal cell, a Purkinje cell and a stellate cell. All nerve cells consist of a soma - a cell body containing the cell nucleus, a quantum of dendrites - the receptive zone of the neuron, and an axon - a nerve fiber that conducts nerve impulses from the soma to other cells. The dendrites typically branch out in larg quantity from one side of the soma, as feathery attachments, to make contact and receive synaptic input from other cells. The axon might be thousands of times longer than the soma itself, and thus it can conduct nerve impulses throughout long distances to nerve cells in other parts of the brain or the body [2][13].

#### 2.1.1 Generation of Action Potentials

The nerve impulse (or action potential), which serves as information transmitter among neurons, is generated due to a change in the voltage gradient across the neuron membrane. The membrane of the nerve cell is filled with ion channels and ion pumps, permeable to certain ions: Mainly sodium ( $\text{Na}^+$ ), potassium ( $\text{K}^+$ ), calcium ( $\text{Ca}^{2+}$ ), and chloride ( $\text{Cl}^-$ ). As these ions ether flow or are pumped in and out of a cell, there will be a change in the voltage gradient (i.e. the difference in electrical potential) between the interior of a neuron and the surrounding extracellular medium. The ion channels open and close in response to voltage changes, which is provoked by signals from other neurons. When the ion consentration inside the cell is in equilibrium with the exterior of the cell, the electrical potential between the

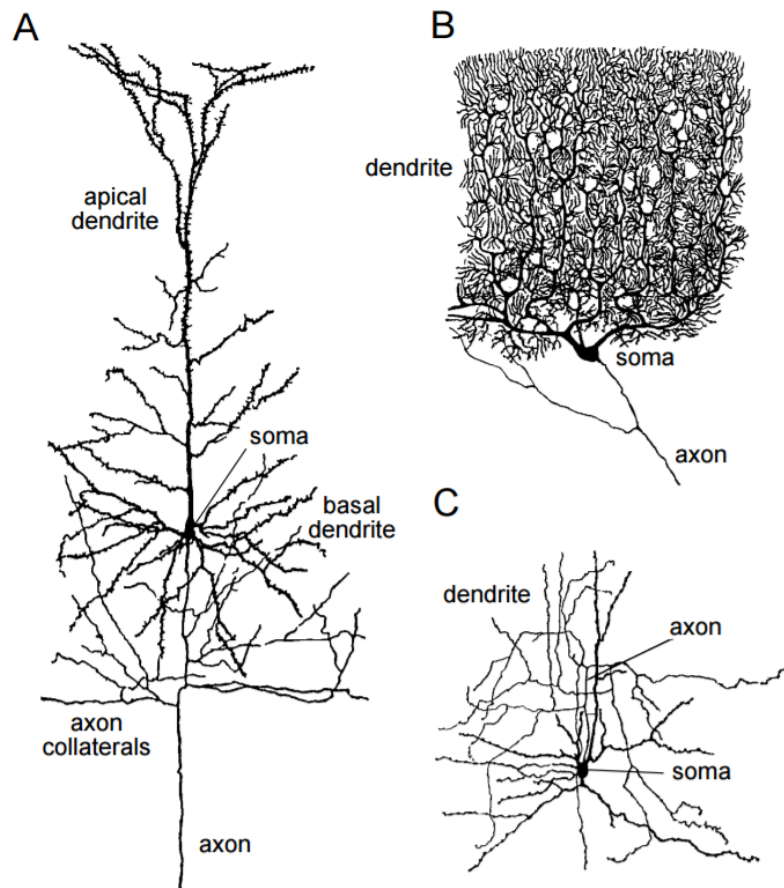


**Figure 2.1:** Example of three neuron types. **A)** A cortical pyramidal cell. They are the most common excitatory neurons in the mammalian cortical structure[?]. A pyramidal cell's axon branch locally to provide feedback to nearby neurons, and also conducts signals longer distances, to other parts of the brain. **B)** A Purkinje cell of the cerebellum. Its dendrites have a great range to receive more information. **C)** A stellate cell of the cerebral cortex. (From Dayan and Abbott's textbook [2]).

interior and the exterior of the cell is called the resting potential, and is about -70 mV. If there is a flow of negatively charged ions into the cell (or a flow of positively charged ions out of the cell), so that the electrical potential turns more negative, the neuron experience hyperpolarizaion. The opposite process, when the membrane potential is changes in the positive direction, the neuron experience a depolarization. There is a threshold level for depolarization before a neuron generates an action potential, usually arround 55 mV. An action potential is a fluctuation in the electrical potential of about 100 mV across the cell membrane, that propagates (is fired) along the axon [2].

### 2.1.2 Signal Transmission Between Nerve Cells

Located at the end of axons are synapses (gap junctions between neurons), containing neurotransmitters. These neurotransmitters are released upon the arrival of action potentials. The neurotransmitters are released from the pre-synaptic (transmitting) cell's axon and defuse the short distance to the post-synaptic (receiving) cell's dendrite. There the neurotransmitters bind to receptors, causing ion channels to open. If the ion flow is of the type that causes depolarisation in the post-synaptic neuron, the synapse has an excitatory effect, and the post-synaptic neuron is more likely to generate an action potential itself. If the ion flow is of the type that causes hyper-polarizing, the synapse have an inhibitory effect on the post-synaptic neuron, and it is less likely to generate an action potential itself. The excitatory effect on neurons encourages signals to be transmitted and spread throughout the brain. The inhibitory feedback is important for the regulation of the signal transmission. Without the inhibition the brain would have uncontrolled signal spreading, similar to that of an epileptic episode.

## 2.2 Early Visual System

The early visual system span all across the brain, and its neurons make connections in such way that make perception of the outside world possible for the brain. This thesis deals with a selection neurons essential for visual stimuli processing. Figure 2.2 illustrates the early visual pathway in the brain, from retina, through the lateral geniculate nucleus (LGN) and to the visual cortex. A schematic view of the neurons and their signalling paths are shown in figure 2.3.

### 2.2.1 Retina

The early visual system begins with the eyes, where light passes through the eye lens and falls upon retina. Retina is filled with rod and cone photoreceptor cells, that

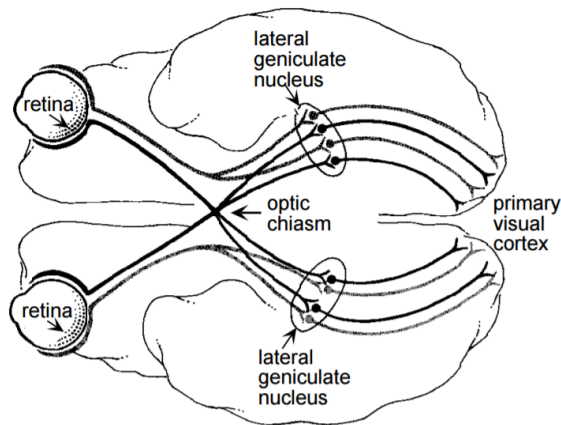


**Figure 2.2:** Pathway from the retina through the lateral geniculate nucleus (LGN) of the thalamus to the primary visual cortex in the human brain. (from Dayan and Abbott's textbook [2]).

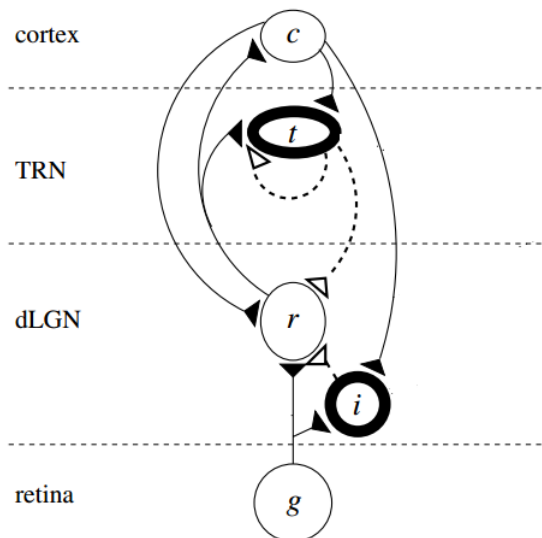


**Figure 2.3:** Schematic view of the geniculate circuit for the X pathway. The neurons involved are retinal ganglion cells ( $g$ ), geniculate relay cells ( $r$ ), intrageniculate interneurons ( $i$ ), thalamic reticular cells ( $t$ ), and cortical cells ( $c$ ). The excitatory connections are shown as solid curves, while the inhibitory connections are shown with dashed curves. (From Einevoll and Plesser, [3]).



converts light into electrical signals. The retinal ganglion cells conduct the signals out of the eye through their axons, which together forms the optic nerve. The retinal ganglion cells conduct the electrical signal to the lateral geniculate nucleus (LGN) in Thalamus, where it synapses onto LGN relay cells and interneurons. The signal transmission from Retinal ganglion cells are excitatory, and so they cause further generation of action potentials for the cells in LGN.

### 2.2.2 Lateral Geniculate Nucleus (LGN)

The LGN is one of several nuclei in Thalamus, which is a sub-cortical structure (i.e. a structure located beneath cortex). It resides in each hemisphere in the middle of the brain. Some ganglion axons cross the midline at the optic chiasm and connect to the LGN in the opposite hemisphere, providing information from both eyes to both sides of the brain. The cellular population of the LGN of a cat consists of 75-80 % relay cells and 20-25 % interneurons [3]. Among interneurons and relay cells, only the latter conduct signals out of the nucleus. Similar to retinal ganglion cells, LGN relay cells make excitatory synapses, and so they relay signals that emerge in retina. LGN relay cells make few intranuclear connections, but synapses on to cells in the thalamic reticular nucleus (TRN) and cells in the primary visual cortex. The local connections in the LGN is dominated by inhibition from interneurons. As interneurons also receive retinal input, and synapse onto each other and relay cells they are said to form a feedforward inhibitory pathway [2][8].

### 2.2.3 Thalamic Reticular Nucleus (TRN)

Another class of inhibitory neurons that suppress the LGN relay cells with inhibition populates the visual sector of the thalamic reticular nucleus (TRN). The TRN is a thin network of interconnected, inhibitory neurons that forms a shell around the dorsal thalamus, and thus the LGN. As TRN cells both receive synaptic input from, and transmit synaptic input to LGN relay cells, TRN cells are said to provide feedback.

### 2.2.4 Visual Cortex

Located in the back of the brain is the visual cortex. Pyramidal cells and spiny stellate cells are densely interconnected with each other in the visual cortex. Local connection apart, cortical cells receive excitation from retina via LGN relay cells, and transmit signals to TRN cells and interneurons of the LGN. Thus, the cortical cells inhibit LGN relay cells indirectly via the TRN cells and the interneurons. In other words the early visual system involves a loop for the visual signal transition, whereas cortical cells are said to provide inhibitory feedback to LGN relay cells. This

feedback contributes to up to 30 % of the input to the LGN. The signal transmission through the cortiothalamic loop (i.e. pathway from LGN to cortex and back) takes between three and ten milliseconds, depending on the pathway [1].

### 2.2.5 Features of LGN

The LGN has been appointed as relay center in the early visual system, but it plays a more complex role in processing of visual stimuli than that. Cortical feedback aside, the LGN does not merely copy retinal input. Visual resolution at the fovea, where retinal ganglion cells receive input from photoreceptive cones, is limited by cone spacing. However, perceptual acuity is greater than what the number of retinal photoreceptors predicts. The explanation for the increased acuity lies in the connections throughout the early visual system: In cat there are twice as many LGN relay cells in LGN as there are retinal ganglion cells in retina. Each ganglion cell diverge to target several relay cells, thereby upsampling the visual resolution. Simulations preformed by Judith A. Hirsch et al. [8] suggest that LGN relay cells receives, on average, input from about three different retinal ganglion cells. Each relay cell achieve a unique combination of retinal input. In this way the the LGN relay cells interpolate retinal input. The result of upsampling and interpolating across the retioenucliate synapse is increased resolution of an image representation that has been smoothed out. This process in thalamus is much alike techniques used in digital image processing.

Finally, neurons are sensitive to contrast boarders, and for reasons to be discussed in the chapter 3, neuron in the LGN sharpen the image representation. So the introduced blur in the upscaled image representation is counteracted[12][8].

## 2.3 Modelling Neurons and Their Network

Neuroscience includes mathematical models of different calibre. They all aim to provide a deeper understanding of the human brain and its functionality. What separates them are their methods. Mechanistic models explain how the functionality of a system arise from the physical properties of the underlying parts. Descriptive models explain evident properties of a system statistically based on experimental data. Finally, interpretive models explain the functional roles of a system. Later on it will become evident that this theses deals with both mechanistic and descriptive models (receptive field models in section 3) [3].

### 2.3.1 Challenges in Computational Neural Network Modelling

When it comes to computational modelling of neurons there are many possibilities regarding detail integration. Single neuron models may take into account details like neuron morphology (soma, dendrites and axon), action potential generating processes (ion concentrations and diffusion across cell membrane), and conductivity (propagation of action potential within the neuron). If this level of detail was included in models of neural network, a computer would have trouble regarding memory storage capability and time consumption, as these models would be extremely computationally expensive. So when modelling neural networks simplifications are needed.

### 2.3.2 Simplifications in Computational Neural Network Modelling

One simplification is to model neurons as simple points and thus neglect the neural morphology. Then the remaining aspect of interest would be the neural connections. Another simplification is to address neural activity in a less complex manner, and neglect the biological process of action potential generating. Neural activity can be modelled as a series of spike times (i.e. times when action potentials were generated), or even simpler: As a firing rate (i.e. number of action potentials per second). When considering firing rates, temporal patterns of action potential firing, which might carry significant information, are lost. However, the use of firing rates is a great way to evaluate which neurons respond to each other in a network. The combination of these two simplifications is called a firing-rate point-neuron model, and will be the basis for the chapters to come.



# Chapter 3

## Receptive Fields

DeAngelis et al. [7] describes receptive fields as follows: "The receptive field is a central construction in the conceptual and analytical framework that is used by neurophysiologists to study the function of visually responsive neurons, because it characterizes the transformation between the visual image and the neuronal activity." [7]. In other words: Receptive field is a commonly accepted concept created to tie visual stimuli to neural response. The concept evolves around the fact that neurons in the retina, LGN and primary visual cortex react to light stimuli within restricted regions of the visual field. These restricted regions are receptive fields, and each individual neuron has its own exclusive receptive field. Neural networks in the early visual system have commonly been modelled by receptive field models. A function that describes the behaviour of receptive fields (i.e. a kernel),  $W(x, y, \tau)$ , are defined in the space-time domain, and ties the neuron response to stimulus at position  $(x, y)$  in the receptive field at time  $\tau$ . The point of peak sensitivity within the receptive field of a cell is the receptive field center. For some neurons the kernel is space-time separable, and can be written as a product of two functions, one that describes the spatial behaviour of the receptive field and the other one that describes the temporal behaviour of the receptive field,  $W(x, y, \tau) = W_s(x, y)W_t(\tau)$  [2].

### 3.1 Modelling of Spatial Receptive Fields

Figure 3.1 A) is an example of a spatial structure of a receptive field, which is approximately spatiotemporal separable. This particular receptive field is determined by the method of spike-triggered average stimuli for a neuron in the primary visual field of a cat. In this case the stimuli were average between 50 ms and 100 ms prior to an action potential. Figure 3.1B is a recreation of the same receptive field fitted by a Gabor function. This figure illustrates an important feature of receptive fields: The ON and OFF regions. The areas where the temporal receptive field function,

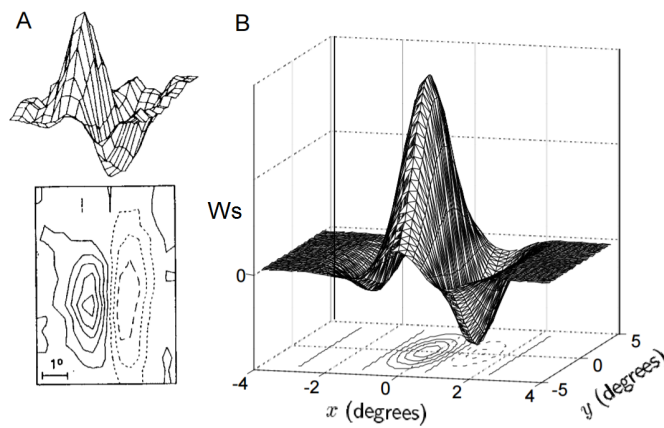


**Figure 3.1:** Spatial receptive fields structure of simple cells. A) Spatial structure of receptive field of a neuron in the primary visual cortex in cat. The upper plot is a three-dimensional representation, with the horizontal direction acting as the x-y plane and the vertical dimension indicating the magnitude and sign of  $W_s(x, y)$ . The lower contour plot represents the x-y plane. Regions with solid contour curves are ON areas where  $W_s(x, y) > 0$  and regions with dashed contours show OFF areas where  $W_s(x, y) < 0$ . B) Construction of a receptive field by the use of a Gabor function with parameters fitted to recreate the receptive field in A). (From Dayan and Abbot's textbook in theoretical neuroscience [2]).

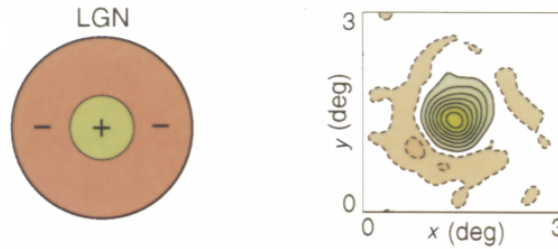


**Figure 3.2:** Schematic and experimental profiles of the receptive field on an ON center LGN neuron of a cat. In the DoG model of the receptive field (left) the receptive field has a centred ON region (+) and a surrounding OFF region (-). The figure to the right illustrates a two-dimensional spatial receptive field profile in the x-y plane for an ON center X-cell, measured using a reverse correlation technique. ON regions are shaded green, and are represented by solide contours. Off regions are shaded red and represented with dashed contours. Colour saturation is porportional to strength. (From Freeman et al. [7].)

$W_s(x, y)$ , is positive are ON regions. The neural response is enhanced when the ON regions are illuminated relative to the background level of illumination. The areas where  $W_s(x, y)$  is negative are OFF regions. The neural response is enhanced when the OFF regions are darkened relative to the background level of illumination. The enhancement (excitation) of neural response when stimulated with the preferred luminance is called "push". Contrarily, suppression (inhibition) caused by darkening an ON region or illuminating an OFF region, is called "pull". As neurons respond to change in luminance contrast, they will react to both the onset and the offset of a stimulus. For example, onset of illumination in a receptive field's ON center causes the push. Offset of illumination in the receptive field's ON center corresponds to darkening, and causes the pull. This is an example of the so called push-pull effect [8].

Elongated receptive fields, like the one seen in figure3.1, show selectivity for edges in the corresponding direction as the receptive field is stretched [8][2]. In contrast to the elongated spatial receptive field of simple cells in the primary visual cortex, the receptive field of retinal ganglion cells and LGN cells has an approximately circular center-surround organization. The center and the concentric ring have the opposite polarities, as illustrated in figure 3.2. The figure show the result of measurement of the receptive field (right) and the corresponding receptive field modelled by a difference-of-Gaussian (DoG) funciton (left). The illustration of the measured receptive field clearly shows a center-surround structure, although the surround is fairly weak. The receptive field seen in the figure illustrate only one of the two forms the center-surround receptive field can take. Figure 3.2 show an ON-center receptive field (i.e. the ON region is in the center). On the other hand there are the OFF-center receptive fields, where the polarities are reversed [7][2]. The circular

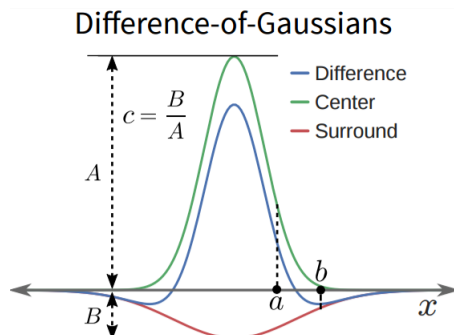


**Figure 3.3:** Two-dimensional view of the Gaussian functions for the excitatory center region and the inhibitory surround region of the spatial receptive field of an ON centered neuron, together with the difference-of-Gaussian function representing the total spatial receptive field. The upper, green line is a Gauss function that illustrates the response function for the excitatory center of the receptive field. The red line is a negative Gauss curve, that illustrates the response function for the inhibitory surround of the receptive field. The blue line in the middle represents the difference of the other two Gaussian functions in the figure,  $W_s(x, y)$ .  $A$  and  $B$  are the amplitudes of the excitation and inhibition, respectively.  $a$  and  $b$  measure the width of the center and surround, respectively. (From Mobarhan [11]).

ON and OFF regions of the receptive fields of LGN relay cells have conventionally been modelled by Gaussian functions since this type of model was introduced by Rodieck in 1965. Now difference-of-Gaussian (DoG) models are used to model responses for neurons in all of the early visual system. DoG models are descriptive models, as their structure are fitted through experiments. The DoG filters are often used in digital image processing for edge detecting, which is the same feature provided by the center-surround receptive fields of neurons in retina and LGN. The difference-of-Gaussian function is described by the following equation:

$$W_s(x, y) = \frac{A}{\pi a^2} e^{-(x^2+y^2)/a^2} - \frac{B}{\pi b^2} e^{-(x^2+y^2)/b^2}. \quad (3.1)$$

A two-dimensional representation of each of the Gauss functions, together with the difference between them are illustrated in figure 3.3. In equation 3.1,  $A$  and  $B$  are the amplitudes of the excitation and inhibition, respectively. The variables  $x$  and  $y$  are the receptive field center's placement in the visual field. The parameters  $a$  and  $b$  represent the width of the center and surround, respectively.

As indicated by the spatial center-surround receptive field structure of retinal ganglion and LGN cells, they respond best to circular spots of light surrounded by darkness (for ON center cells) or to dark spots surrounded by light (for OFF center cells). However, if for example a spot of light on the ON-center cell expands to fill



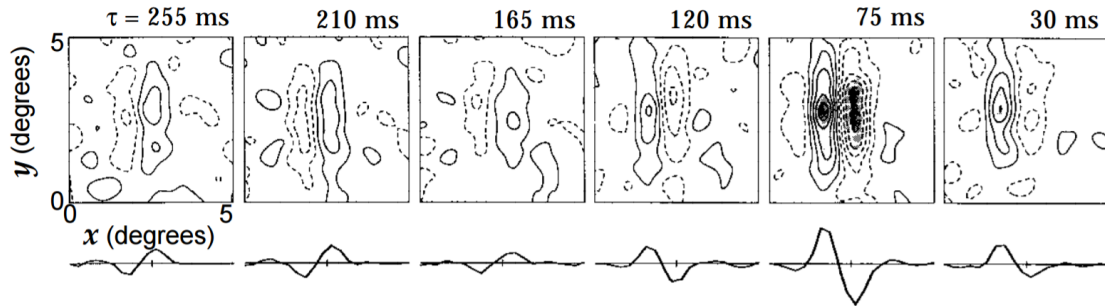
the surround as well as the center, the push mechanism is put into effect. This will suppress the excitation of the cell. This effect allows for edge detecting and reduces response to diffuse or homogeneous patterns. The image sharpening tendency of the LGN derive from the fact that the pull area exceeds the push area for relay cells whose receptive fields lie within the central 10-15 degrees of visual space. Thus the relay cells are more easily inhibited than excited, and are less likely to fire close to messy edges.

## 3.2 Modelling of Temporal Receptive Fields

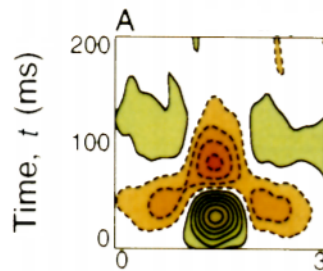
Receptive field illustrations like the one in figure 3.3 embody only the spatial aspect of the receptive field structure. However, the organization of the receptive field is not static. The spatial structure of the receptive field of most neurons changes as a function of time, and must therefore be characterized in the space-time domain. The temporal aspect of receptive fields is far less studied than the spatial. Only recently have there been developed techniques to analyze the spatiotemporal characteristics of neural receptive fields.

Figure 3.4 shows a series of snap shots of the spatial receptive field of a neuron in the primary visual cortex of a cat. The frames reveal the temporal development of the neural receptive field. There is little correlation between the visual stimulus and the upcoming spike more than 300 ms prior to the spike. In the early frame that shows the spatial receptive field 255 ms prior to the spike, the ON and OFF regions of the receptive field, similar to the one in figure 3.1, are evident. As the time approaches the spike time ( $\tau = 0$ ) this structure fades and reverses. The spatial receptive field 75 ms prior to the spike time is reversed compared to at 210 ms prior to the spike time. Thus, this cell is reactive to an aligned dark-light boundary that reverts to a light-dark boundary with time. This is a so called reversal effect, and it is common in temporal receptive fields. Worth pointing out is the fact that even though the signs of the different spatial regions change with time, their locations and shapes remain fairly unchanged. This makes the receptive field in figure 3.4 space-time separable [7][2].

Figure 3.5 illustrates another way of visualising the dynamics of the receptive field structure. From the x-t plot the one-dimensional spatial organisation as a function of time is clear. The plot is constructed by obtaining one-dimensional profiles of the spatial structure at finely spaced time intervals (5-10 ms) over a range of time values. The one-dimensional profiles are then stacked up to form a surface, that is plotted as a contour map. The contour map in figure 3.5 shows an ON center LGN cell of a cat. This x-t plot shows deviation from separability, even though LGN cells are approximated to be space-time separable. The temporal response of the surround region is delayed slightly compared to the center region. Although the reversal effect



**Figure 3.4:** Temporal evolution of a spatial receptive field. Each frame is a plot of  $W_s(\vec{r}, \tau)$  for different times,  $\tau$ , prior to the firing of an action potential. Regions with solid contour curves are ON areas where  $W_s(x, y) > 0$  and regions with dashed contours show OFF areas where  $W_s(x, y) < 0$ . The curves below the contour diagrams are one-dimensional plots of the receptive field as a function of  $x$  alone. The receptive field is maximally different from zero for  $\tau = 74$  ms with the spatial receptive field reversed from what it was at  $\tau = 210$  ms. (Figure and caption adapted from Dayan and Abbot's textbook in theoretical neuroscience [2]).



**Figure 3.5:** Spatiotemporal receptive field profile ( $x$ - $t$  plots) for a ON center X-cell in the LGN of a cat. The horizontal axis represents space in the  $x$ -direction, and the vertical axis represents time. Solid contours with green shading indicate ON regions, whereas broken contours with red shading indicate OFF regions. For  $t < 50$  ms, the receptive field has an ON center and an OFF surround region. However, for  $t > 50$  ms, the receptive field center becomes an OFF region, and the surround becomes an ON region. (Figure and caption adapted from DeAngelis et al. [7]).

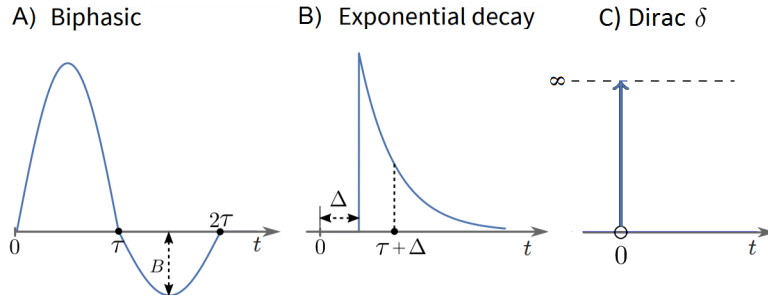


**Figure 3.6:** A) Biphasic, B) exponential decay, and C) Dirac  $\delta$ -function. These functions are used to model receptive field dynamics. Figure provided by Milad Mobarhan and adapted in paint.

is evident, as the polarity of the regions in the receptive field switch after about 50 ms. Temporal reversal effect seen in figure 3.4 and 3.5, can be described by the following biphasic function:

$$W_{t,\text{biphasic}}(t) = \begin{cases} \sin(\pi t/a) & 0 \leq t \leq a \\ B\sin(\pi t/a) & a \leq t \leq 2a \\ 0 & \text{otherwise.} \end{cases} \quad (3.2)$$

The biphasic function is illustrated in figure 3.6 A. The parameter  $B$  is a damping factor in the form of a positive number smaller than one, and  $a$  is the duration of each phase of the signal. For example, the phase duration of the signal illustrated in figure 3.5 is about 50 ms. Other temporal kernels used in modelling neural networks are the Dirac  $\delta$ -function and the exponential decay function:

$$W_{t,\text{delta}}(t) = \delta(t - \Delta) \quad (3.3)$$

$$W_{t,\text{decay}}(t) = e^{-(t-\Delta)/\tau} \theta(t - \Delta) / \tau. \quad (3.4)$$

The Dirac  $\delta$ -function and the exponential decay function are illustrated in figure 3.6 B and C, respectively.  $\theta(t)$  is the Heaviside step function.  $\tau$  is the time constant and  $\Delta$  is the delay. The biphasic, the  $\delta$ - and the exponential decay functions are all used for the simulation of an early visual system network in chapter 5.



## Chapter 4

# The Mathematical Model (eDoG for LGN Circuits)

The mathematical model behind the simulations in this thesis is the extended difference-of-Gaussian (eDoG) model, introduced by Einevoll and Plesser [6]. The eDoG model is a mechanistic, linear, point-neuron model, that links the firing rate of LGN relay cells to visual stimuli. The model is named after the mathematical function it applies to describe the spatial aspect of neural receptive fields: The difference-of-Gaussian function. The model has been designed to explore the effect of cortical feedback on the response of LGN relay cells. The advantage of the eDoG model is its efficiency. Possible effects of cortical feedback on LGN cells can be studied more easily than with extensive numerical simulations of neural networks.

### 4.1 Impulse-Response Function

The general accepted equation for relating the linear cell response to visual stimulus in computational neurophysics is given by

$$R(\vec{r}, t) = \int_{\tau} \iint_{\vec{r}_0} W(\vec{r} - \vec{r}_0, \tau) S(\vec{r}_0, t - \tau) d^2 \vec{r}_0 d\tau. \quad (4.1)$$

The neural response,  $R(\vec{r}, t)$ , is related to the stimulus by the impulse-response function,  $W(\vec{r}, \tau)$ . The impulse-response function determines how strongly, and with what sign, the visual stimulus,  $S(\vec{r}, t)$ , at point  $\vec{r} = (x, y)$  and time  $t - \tau$  affects the firing rate of the neuron at time  $t$ . Thus the impulse response function is closely connected to the receptive field function. In fact, the impulse-response function is the mirrored version of the receptive field function,  $F(\vec{r}) = W(-\vec{r})$  [6]. The spatial integral of equation 4.1 sums the contributions to the neural response over

all to-dimensional space. The temporal integral sums the contributions to the neural response from negative infinity to positive infinity ( $\tau = -\infty$  to  $\tau = \infty$ ) to satisfy the general expression of the Fourier transform. The lower integration boundary could as well have been set to zero, as it follows from causality that  $W(\vec{r}, \tau < 0) = 0$ . The equation assumes linearity; it holds for neurons where the contributions from different locations within the visual fields sum in a linear matter. This is the case for e.g. the X-cell in the cat retina and LGN, and simple cells in primary visual cortex. Equation 4.1 is a convolution between the impulse-response function and the stimulus, i.e.

$$R(\vec{r}, t) = W(\vec{r}, t) \otimes S(\vec{r}, t). \quad (4.2)$$

The Fourier transform of equation 4.1:

$$R(\vec{r}, t) = \frac{1}{2\pi^3} \int_{\omega} \int_{\vec{k}} e^{-i(\vec{k}\vec{r}-\omega t)} \tilde{W}(\vec{k}, \omega) \tilde{S}(\vec{k}, \omega) d^2\vec{k} d\omega. \quad (4.3)$$

$\tilde{W}(\vec{k}, \omega)$  and  $\tilde{S}(\vec{k}, \omega)$  are the Fourier transformed impulse-response function and stimulus, respectively. The firing rate,  $R(\vec{r}, t)$ , is an infinite sum over the drifting, sinusoidal gratings specified by the wave vector,  $\vec{k}$ , and the angular frequency,  $\omega$ . The wave vector is related to the spatial frequency via  $|\vec{k}| = 2\pi\nu$ . The angular frequency is related to temporal frequency via  $\omega = 2\pi f$ . The complex Fourier transformed used for the transformation, and its inverse, are given by

$$\tilde{y}(\vec{k}, \omega) = \int_t \int_{\vec{r}} e^{-i(\vec{k}\vec{r}-\omega t)} y(\vec{r}, t) d^2\vec{r} dt, \quad (4.4)$$

$$y(\vec{r}, t) = \frac{1}{(2\pi)^3} \int_{\omega} \int_{\vec{k}} e^{i(\vec{k}\vec{r}-\omega t)} \tilde{y}(\vec{k}, \omega) d^2\vec{k} d\omega. \quad (4.5)$$

## 4.2 Coupling Function

Neural response to input from another cell, as opposed to response to visual stimuli, can be described as a convolution analogue with equation 4.1,

$$\begin{aligned} R_m(\vec{r}, t) &= \int_{\tau} \int_{\vec{r}_0} K_{mn}(\vec{r} - \vec{r}_0, \tau) R_n(\vec{r}_0, t - \tau) d^2\vec{r}_0 d\tau \\ &= K_{mn}(\vec{r}, t) \otimes R_n(\vec{r}, t), \end{aligned} \quad (4.6)$$

with  $K_{mn}(\vec{r}, t)$  corresponding to the impulse-response function and  $R_n(\vec{r}, t)$  corresponding to the stimuli.  $R_m(\vec{r}, t)$  and  $R_n(\vec{r}_0, t - \tau)$  are the impulse-response functions

of cell  $m$  and  $n$ , respectively.  $\tilde{K}_{mn}(\vec{r}, t)$  is the coupling function, which describes the transfer ratio from cell  $n$  to cell  $m$ . Equation 4.6 is Fourier transformed in the same manner as shown above for equation 4.1.

### 4.3 The Geniculate Transfer Function

Einevoll and Plesser [5] introduce an important relation between a neuron's impulse-response function and the coupling functions for the connected cells. This was done by introducing a function for a drifting grating pattern of luminance as  $\tilde{S}(\vec{k}, \omega)$  in equation 4.3 for a retinal ganglion cell. Further the result of the equation for the ganglion cells response was introduced into the Fourier transformed version of the equation 4.6 for relay cell response. By comparing this calculation of relay cell response with equation 4.3 for a relay cell response to visual stimulus, the relation becomes evident. The transfer ratio from a ganglion cell to a relay cell is only dependent of the coupling function  $\tilde{K}_{rg}(\vec{k}, \omega)$ . As this will hold for the connection between all the cells in the early visual system, the more general relationship can be stated:

$$\tilde{W}_m(\vec{k}, \omega) = \tilde{T}_{mn}(\vec{k}, \omega) \tilde{W}_n(\vec{k}, \omega) \quad (4.7)$$

Where  $\tilde{T}_{mn}(\vec{k}, \omega)$  is the geniculate transfer function. The transfer function is dependent only of the coupling functions between the connected cells, rather than their impulse-response functions.

### 4.4 Coupling Scheme

The derivation of the geniculate transfer function,  $\tilde{T}_{rg}(\vec{k}, \omega)$  between retinal ganglion cell and LGN relay cells is based on knowledge of the neuronal connectivity in the LGN. Einevoll and Plesser [6] modify the neural connections shown in figure 2.3 into the connections shown in figure 4.1. The neurons in the latter figure reflect neuron populations, and the coupling function for each connection is stated. Figure 4.1 illustrates that the feedforward inhibitory input from the LGN interneuron to the relay cell is regarded as an indirect inhibition from the retinal ganglion cell. Thus the ganglion cells are considered to provide both excitatory and inhibitory input to the relay cell. Pathways from two ganglion cells, one ON-center and one OFF-center, are included to emphasize the cross connection between cortical and relay cells. The cortical cell populations provide both excitatory feedback and indirect inhibitory feedback, as described in section 2.2.4. As mentioned in chapter 3.1, the spatial receptive field of a simple cortical cell, as the one in figure 3.1, imply that

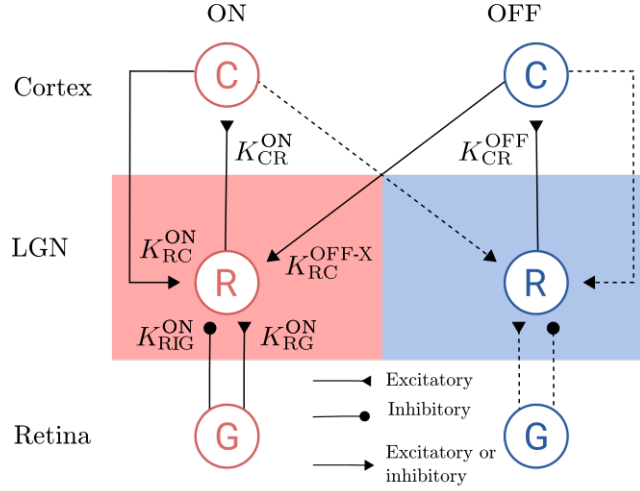


**Figure 4.1:** Schematic view of the simplified geniculate circuit for ON-cells and OFF-cells in the eDOG model. The neurons involved are retinal ganglion cells (G), geniculate relay cells (R), and cortical cells (C). Figure collected from Mobarhan’s documentation, [9].

cortical cells are orientation selective (i.e. they respond more significant to a stimulus with a specific orientation). The eDOG model consider a set of  $N$  mutually uncoupled, orientation-selective cortical populations  $C_n$ , for  $n = 1, 2, \dots, N$ . They respond preferably to stimuli with orientation  $\theta_n$ . Based on the impulse-response function, the coupling function and the constructed representation of neural connectivity presented in figure 4.1, Einevoll and Plesser (2012) [6] present the following coupling scheme for response of ON-center neurons in the early visual system:

$$\begin{aligned}
 R_g^{\text{ON}}(\vec{r}, t) &= W_g^{\text{ON}}(\vec{r}, t) \otimes S(\vec{r}, t) \\
 R_c^{\text{ON}}(\vec{r}, t) &= K_{c_n r}^{\text{ON}}(\vec{r}, t) \otimes R_r^{\text{ON}}(\vec{r}, t) \\
 R_r^{\text{ON}}(\vec{r}, t) &= K_{r_g}^{\text{ON}}(\vec{r}, t) \otimes R_g^{\text{ON}}(\vec{r}, t) \\
 &+ K_{r_{\text{rig}}}^{\text{ON}}(\vec{r}, t) \otimes R_g^{\text{ON}}(\vec{r}, t) \\
 &+ \sum_n K_{r_{c_n}}^{\text{ON}}(\vec{r}, t) \otimes R_{c_n}^{\text{ON}}(\vec{r}, t) \\
 &+ \sum_n K_{r_{c_n}}^{\text{OFF-X}}(\vec{r}, t) \otimes R_{c_n}^{\text{OFF}}(\vec{r}, t).
 \end{aligned} \tag{4.8}$$



In this set of equations  $R_g$ ,  $R_r$  and  $R_{c_n}$  are the responses of retinal ganglion cells, relay cells, and cortical cells, respectively.  $S(\vec{r}, t)$  represents the visual stimulus.  $K_{jk}^{\text{ON}}(j, k : g, r, c_n)$  is the linear, spatiotemporal coupling function from ON-neurons of type  $k$  onto ON neurons of type  $j$ . The coupling function decides how the firing rate of cell type  $k$  at position  $r_0$ , and time  $t = 0$  affects the firing rate of cell type  $j$  at position  $\vec{r}$  a time  $\tau$  later. The coupling function  $K_{\text{rig}}^{\text{ON}}$  represents the indirect signal from ON ganglion cells, via interneurons, onto ON relay cells.  $K_{rc_n}^{\text{OFF-X}}$  represents the cross-coupling feedback from cortical OFF cells onto relay ON cells. This set of equations is the basis for the derivation of the LGN relay cell impulse response function,  $\tilde{W}_r^{\text{ON}}$  [6].

## 4.5 Impulse-Response Function of LGN Relay Cells

Einevoll and Plesser [6] make three assumptions in order to derive an impulse-response function for the LGN relay cell: Firstly the response functions for the cortical cells are half-wave rectified functions, so that

$$R_{c_n}^{\text{ON}}(\vec{r}, t) = [K_{c_n r}^{\text{ON}} \otimes R_r^{\text{ON}}(\vec{r}, t)]_+. \quad (4.9)$$

Secondly the input to the half-wave rectifying function for the cortical OFF cell is exactly the negative of the input to the half-wave rectifying function for the cortical ON cell,

$$R_{c_n}^{\text{OFF}}(\vec{r}, t) = [-K_{c_n}^{\text{ON}} \otimes R_{c_n}^{\text{ON}}(\vec{r}, t)]_+ \quad (4.10)$$

Thirdly the cross-connected feedbacks from the ON and OFF cortical cells are phase-reversed,

$$K_{rc_n}^{\text{OFF-X}} = -K_{rc_n}^{\text{ON}}. \quad (4.11)$$

Using these assumptions and the mathematical identity  $[x]_+ - [-x]_+ = x$  on the coupling scheme in section 4.4, Einevoll and Plesser (2012) derive the following equation for LGN relay impulse-response functions [6]:

$$\begin{aligned} \tilde{W}_r^{\text{ON}} &= \tilde{T}_{\text{rg}}^{\text{ON}}(\vec{k}, \omega) \tilde{W}_g^{\text{ON}}(\vec{k}, \omega) \\ &= \frac{\tilde{K}_{\text{rg}}(\vec{k}, \omega) + \tilde{K}_{\text{rig}}(\vec{k}, \omega)}{1 - \sum_{n=1}^N \tilde{K}_{rc_n}^{\text{ON}}(\vec{k}, \omega) \tilde{K}_{c_n r}^{\text{ON}}(\vec{k}, \omega)}. \end{aligned} \quad (4.12)$$

The first and second term of the numerator represent the direct feedforward excitation from retinal ganglion cells and the indirect feedforward inhibition via interneurons, respectively. The sum in the denominator represents the corticothalamic loop formed of all  $N$  cortical populations.

As mentioned in chapter 3.1, simple cortical cells have elongated spatial receptive fields, and they are not spatiotemporal separable. Although this is the case for the individual contribution of the sum, Einevoll and Plesser [6] argue for the possibility of considering the sum as a whole as spatiotemporal separable. They point out that if there were infinitely many cortical populations,  $N = \infty$ , with orientation preference  $\theta_n$ , the sum of their receptive fields would include all 360 degrees of orientation preference, and thus be circular symmetric. So the sum in the denominator of equation 4.12 can be regarded as a circular, spatiotemporal separable receptive field, equal to those of retinal ganglion and LGN relay cells. Even though no particular cortical population responds strongly to a circular spot, all cortical populations respond to some extent, and the sum of the many small responses from the total number of cortical populations, will contribute to an overall significant cortical feedback effect. Equation 4.12 can then be rewritten as

$$\tilde{W}_r(\vec{k}, \omega) = \frac{\tilde{K}_{\text{rg}}(\vec{k}, \omega) + \tilde{K}_{\text{rig}}(\vec{k}, \omega)}{1 - \tilde{K}_{\text{rcr}}(\vec{k}, \omega)} \tilde{W}_g(\vec{k}, \omega), \quad (4.13)$$

where  $\tilde{K}_{\text{rcr}}(\vec{k}, \omega)$  is the summed loop (i.e. pathway from LGN to cortex and back) coupling function of all cortical populations. In this equation all coupling functions are spatiotemporal separable, so that each coupling function can be written as a product of a spatial and a temporal factor:  $\tilde{K}(\vec{k}, \omega) = \tilde{f}(\vec{k})\tilde{h}(\omega)$ . Finally, Einevoll and Plesser [6] merge the direct excitatory coupling function  $\tilde{K}_{\text{rg}}$  with the indirect inhibitory coupling function  $\tilde{K}_{\text{rig}}$ . The result is a coupling function that contributes with both push (directly from the ganglion cell) and pull (indirectly via the interneuron). The final equation for the impulse-response function of the relay cell is given by

$$\tilde{W}_r(\vec{k}, \omega) = \frac{\tilde{f}_{\text{ff}}(\vec{k})\tilde{h}_{\text{ff}}(\omega)}{1 - \tilde{f}_{\text{fb}}(\vec{k})\tilde{h}_{\text{fb}}(\omega)}. \quad (4.14)$$

In this equation the spatial and temporal part of the contribution (both push and pull) from the ganglion coupling functions is given by  $\tilde{f}_{\text{ff}}(k)$  and  $\tilde{h}_{\text{ff}}(\omega)$ , respectively. The spatial and the temporal part of the contribution (both push and pull) from the coupling function for all cortical populations is given by  $\tilde{f}_{\text{fb}}(k)$  and  $\tilde{h}_{\text{fb}}(\omega)$ , respectively. The new coupling functions are labelled "ff" and "fb" for "feedforward" and "feedback", respectively. Equation 4.14 is the foundation for the simulation tool that will be used later on in this thesis.

# Chapter 5

## Simulation

Study of the cortical feedback's influence on LGN relay cell response is currently being performed at Centre for Integrative Neuroplasticity (CINPLA). PhD candidate Milad Mobarhan at CINPLA has recently developed a simulation tool based on Einevoll and Plesser's mathematical eDoG model, to aid this research. The simulation tool has been the foundation for the study of temporal aspects of cortical feedback in this thesis.

### 5.1 Programming Tools

The following sections briefly explain the general programming tools that has been used for this thesis.

#### 5.1.1 Python

Python is an interpreted, object-oriented, high-level programming language. The advantage with Python is its simple syntax, which emphasizes readability and increased productivity. Also, programme code written in python is easier to access for the general scientific user, without too much experience with more low-level programming. Python supports modules and packages, which encourages program modularity and code reuse. The Python interpreter and the extensive standard library are available without charge for all major platforms. Python version 3.6.0 was used for this thesis.

#### 5.1.2 Spyder

Spyder is an open source, cross-platform integrated development environment (IDE) for scientific programming in Python. It has advanced editing, interactive testing,

debugging and introspection features. Spyder integrates commonly used libraries such as matplotlib (interactive 2D/3D plotting), NumPy (linear algebra) and SciPy (signal and image processing), along with IPython (interactive computing command shell), and other open source software. Spyder is included in certain Python scientific distributions, for example Anaconda. Spyder version 3.1.2 was used for this thesis.

### 5.1.3 Anaconda

Anaconda is an open data science platform powered by Python. It is a Python distribution and a package and environment manager, which includes many of the most popular Python packages for data science. An advantage with Anaconda is that it is a multi platform, and can be used with ease whether on all operative systems Windows, macOS or Linux. Anaconda version 4.3.1 was used for this thesis.

### 5.1.4 GitHub

Git is a version control system (VCS) for tracking changes in computer files, and coordinating work on files among multiple people. GitHub, a web-based Git, was used for this thesis. An advantage of GitHub is that it offers all of the distributed version control and source code management functionality of Git, but also provide its own features: Access control and several collaboration features such as bug tracking, feature requests, task management, and wikis for projects. The source code for the neural circuit simulation tool by Milad Mobarhan is available on GitHub [11]. Also, the application of pylgn that provides this thesis' results is available on GitHub [14].

## 5.2 Neural Circuit Simulation Tool (pylgn)

The LGN simulator is a firing-rate based, visual stimulus-driven simulator of spatiotemporal cell responses in LGN. The mathematical model behind this simulator is Einevoll and Plesser's eDoG model from section 4. The LGN simulator is an open source software, available on GitHub [11] for both C++ (lgn-simulator) and Python (pylgn). For this thesis the python version of the simulator was used. The application programming interface (API) for pylgn is found in the source code documentation [10], together with installation instructions. The network created to study temporal aspects of cortical feedback with pylgn will be discussed, after a simple example application is provided.

### 5.2.1 Example Application

This section illustrates the application of pylgn with a simple example. A modest network consisting of two cell populations is constructed. It is assumed spatiotemporal separable receptive fields for the neurons. The first step in implementing pylgn is to create a network, which is done in the following way:

```
import pylgn
import pylgn.kernels.spatial as spl
import pylgn.kernels.temporal as tpl

network = pylgn.Network()
```

**Listing 5.1:** Python code for creating a network with pylgn

The code above imports the pylgn package, including the spatial and temporal modules. The created network (named "network" in this case) is an object that contains classes for creating and containing neuron, kernel and stimuli objects. The next step in the implementation of pylgn is to create an integrator, as computational physicist's computer simulations often include. The purpose of an integrator is to numerically integrate the contributions from inputs that are only calculated at discrete points. In pylgn the integrator defines a spatial grid of a visual field, which the contributions from stimuli are integrated over for space and time. The code below generates an integrator with  $2^{nt}$  and  $2^{ns}$  spatial and temporal points, respectively. The temporal and spatial resolutions are determined by dt and dr, respectively. If units are not given the resolution arguments, "milliseconds" and "degrees" are used by default for dt and dr, respectively. The integrator is constructed the following way:

```
integrator = network.create_integrator(nt=5, nr=7,
                                       dt=1, dr=0.1)
```

**Listing 5.2:** Python code for creating the integrator with pylgn

Further, neurons can be added to the network using the network's `create_*` methods. The available neurons already implemented in pylgn are retinal ganglion cell, LGN relay cell and cortical cell. Their attributes can be reviewed in pylgn's documentation [10]. For the ganglion cell, which unlike the other neurons receives visual stimulus (as explained in chapter 2.2.1) the impulse-response function is given as an argument. In the example below, the spatial and temporal impulse-response functions,  $W_{g,s}$  and  $W_{g,t}$  are given as arguments. If no arguments are given the default factors of the impulse-response function are a spatial DoG function and a temporal Dirac  $\delta$ -function. Neuron's attributes are stored in a dictionary in the neuron objects. Printing, for example, "vars(ganglion)" in the Spyder console displays the attributes for the ganglion cell. A relay and a ganglion cell are constructed the following way:

```

ganglion = network.create_ganglion_cell(kernel=(Wg_s, Wg_t))
relay = network.create_relay_cell()

```

**Listing 5.3:** Python code for creating a ganglion cell and a relay cell with pylgn

Kernels can also be added to the network using `create_*` methods. The available spatial kernels already implemented in pylgn are Gauss, difference of Gaussian (DoG) and Dirac delta. The available temporal kernels are Dirac delta, biphasic and exponential decay. One can create and implement new kernels using the programming function given in the plgn documentation [10] in the kernel section. The example below creates a temporal and a spatial kernel for the coupling between ganglion cell and relay cell. The network method `connect()` assigns kernels to their respective neuron connection. The method has the following signature: `connect(source, target, kernel, weight)`, where "source" and "target" are the source and target neurons, respectively. The argument "kernel" is the coupling function, and "weight" is the connection weight (default is `weight=1`). If a separable coupling function is implemented then a tuple consisting of the spatial and temporal part is given as the "kernel" argument. Kernels are constructed and assigned in the following way:

```

Krg_r = spl.create_dog_ft()
Krg_t = tpl.create_delta_ft()

network.connect(ganglion, relay, (Krg_r, Krg_t))

```

**Listing 5.4:** Python code for creating coupling functions and connecting neurons with pylgn

The kernel parameters are stored in dictionaries among all other neuron attributes in the neuron objects. The neuron attribute dictionary is quite long, therefore it is more convenient to simply show a part of it. When writing into the Spyder console `"print(pylgn.closure_params(k))"`, where `k` is a random kernel, a print showing the parameters of `k` is displayed. An example print of a dictionary with kernel parameters is seen in the box right below. The kernel used for the print was the DoG coupling function  $K_{rg,r}$  from above.

```

{'center': {'params': {'A': 1, 'a': array(0.62) * deg},
            'type': 'create_gauss_ft'},
 'surround': {'params': {'A': 0.85, 'a': array(1.26) * deg},
              'type':
                'create_gauss_ft'}}

```

**Listing 5.5:** Print of dictionary containing DoG kernel parameters

Last thing to be integrated in the network is the stimulus - this is not necessary if one study only the impulse response function of a network, as the impulse response is independent of stimulus. Stimulus is added to the network using the network's `stimulus.create_*` methods. A full-field grating stimulus, like the one created below, has several parameters, including angular frequency  $\omega$ , wave number,  $k$ , orientation,  $\theta$ , and contrast,  $c$ . The contrast is not set in this example, and it will therefore be set to the pylgn's predefined default value,  $c = 1$ . All kernels in the network will be Fourier transformed according to the transformation in section 4.1 when computing the impulse-response or the response of a cell with pylgn. This is also the case for the stimulus. When using the analytical expression for the Fourier transform of the grating stimulus, it is necessary to make sure that the chosen angular and spatial frequencies exists within the transformed grid. The temporal and spatial frequencies are determined by the number of points and resolution set in the integrator. A simple way of choosing frequencies is to adapt values that has already been created in the Fourier transformation of the integrator. This is done by collecting the desired frequency element from the integrator's lists "spatial\_freqs" and "temporal\_freqs" of transformed spatial and temporal frequencies, respectively. In the example below element "3" and "1" are chosen from the spatial\_freqs list and the temporal\_freqslists, respectively.

```
k_g = integrator.spatial_freqs[3]
w_g = -integrator.temporal_freqs[1]

stimulus = pylgn.stimulus.create_fullfield_grating_ft
           (angular_freq=w_g, wavenumber=k_g, orient=0.0)

network.set_stimulus(stimulus)
```

**Listing 5.6:** Python code for creating stimulus with pylgn

Finally the relay cell response can be computed. The code in the box below computes the response of the LGN relay cells, and animate the activity over time:

```
network.compute_response(relay)
pylgn.plot.animate_cube(relay.response)
```

**Listing 5.7:** Python code for computing LGN relay cell response and make an animated plot with pylgn

### 5.2.2 Create Network

A bigger network than the one in the example above is needed to study the impact of cortical feedback on the LGN relay cells. Spatiotemporal summation curves were

made with `pylgn` to study temporal aspects of cortical feedback. For this purpose the integrator arguments were set to  $nt = 10$ ,  $nr = 7$ ,  $dt = 1$ ,  $dr = 0, 1$ . Thus this is a grid with with  $2^{10} = 1024$  temporal points and  $2^7 = 128$  spatial points. As the spacing is 0,1 degree for the spatial points and 1 ms for the temporal points, the grid reaches over 12,8 degrees in each directions for 1024 ms. This resolution will be sufficient to see trends when responses are plotted.

### 5.2.3 Create Neurons

It was necessary to create more neurons than in the example to study cortical feedback. As mentioned in section 4.5, and as established by equation 4.14, the signals from LGN interneurons and TRN cells are considered as a part of the feedforward contribution from ganglion cells and feedback from cortical cells. For this reason they do not need to be created as neurons, but as additional pull features of the coupling functions. To study cortical feedback it will be necessary to create a population of retinal ganglion cells, LGN relay cells and cortical cells. For the purpose of studying temporal delay effects for excitation and inhibition separately, two populations of cortical cells were created and assigned separate coupling functions. One cortical cell will represent the excitation and the other the inhibition of the cortical feedback. The excitation derive from the direct feedback from the cortical cell population itself, while the inhibition derive from the indirect feedback via the the interneuron and the TRN cell populations - remember the coupling scheme in figure ?? in section 2.2. The advantage gained by separating excitation and inhibition of the cortical feedback is the opportunity to vary their parameters separately. It is reasonable to assume that the inhibitory feedback will be delayed compared to the excitatory feedback, as a result of synapses via interneurons and TRN cells. The neurons in the main network were created by implementation of `pylgn` as showed below:

```
ganglion = network.create_ganglion_cell()
relay = network.create_relay_cell()
cortical_exci = network.create_cortical_cell()
cortical_inhi = network.create_cortical_cell()
```

**Listing 5.8:** Python code for creating neurons for the main network with `pylgn`

The two neurons are labelled "exci" and "inhi", as one represents the excitatory and inhibitory cortical feedback. From now on they will be referred to as "excitation cell" and "inhibition cell".



### 5.2.4 Choice of Coupling Functions and Parameters

The kernels used to form the main network is given in the following programme code:

```
# create spatial kernels
Wg_s = spl.create_dog_ft(A=1.00, a=0.62 *pq.deg,
                        B=0.85, b=1.26 *pq.deg)

Krg_s = spl.create_gauss_ft(A=1, a=0.1*pq.deg)
Kcr_s = spl.create_delta_ft()
Krcr_exci_s = spl.create_gauss_ft(A=1, a=(0.1) *pq.deg)
Krcr_inhi_s = spl.create_gauss_ft(A=2, a=(0.9) *pq.deg)

# create temporal kernels
Wg_t=tpl.create_biphasic_ft(phase_duration =42.5 *pq.ms,
                           damping_factor =0.38,
                           delay =0 *pq.ms)

Krg_t = tpl.create_exp_decay_ft(18 *pq.ms, delay = 1 *pq.ms)
Kcr_t = tpl.create_delta_ft()
Krcr_exci_t = tpl.create_exp_decay_ft(1 *pq.ms,
                                       delay = 2 *pq.ms)
Krcr_inhi_t = tpl.create_exp_decay_ft(1 *pq.ms,
                                       delay = 20 *pq.ms)
```

**Listing 5.9:** Python code for creating the impulse-response function and coupling functions for the main network with pylgn

As seen in the box above, the spatial part of the impulse-response function for the ganglion cell,  $W_{g,s}$ , has been modelled as a spatial DoG, given by equation 3.1. The parameters for the DoG functions,  $A = 1.00, a = 0.62, B = 0.85, b = 1.26$ , are adapted from Mobarhan [10]. The temporal part of the impulse-response function,  $W_{g,t}$ , has been modelled as a biphasic function, given by equation 3.2. The parameters for the biphasic function,  $a = 0.42.5$  ms and  $B = 0.38$ , were adapted from Nordheim et. al. [16]. The box above shows that the kernel representing the connection between ganglion and relay cell has been modelled as a spatial Gauss function described by the first part of equation 3.1, and a temporal exponential decay function from equation 3.4. The kernels  $K_{rcr,exci,s}$  and  $K_{rcr,exci,t}$  specify the thalamo-cortico-thalamic loop for the excitatory cell. The kernels  $K_{rcr,inhi,s}$  and  $K_{rcr,inhi,t}$  specify the thalamo-cortico-thalamic loop for the inhibitory cell. The spatial kernels for the center and surround cell were modelled as Gauss functions, which correspond to the first (center) and second (surround) part of equation 3.1. The box above shows that the spatial parameters are set to  $A = 1, a = 0.1$  for the excitatory cell and

$A = 2$ ,  $a = 0.9$  for the inhibitory cell. The temporal kernels for the excitatory and inhibitory cell were modelled as exponential decay functions from equation 3.4. The time constant,  $\tau$ , is set to 1 for both the center cell and the surround cell. The delays that are displayed in the box above are set to 2 ms and to 20 ms for the center and the surround, respectively. The delay parameters are varied to obtain different spatiotemporal summation curves. As mentioned in section 2.2.4, the loop has a time window between three to ten seconds, the delay parameter used to create the summation plots represent an extreme value. This is chosen intentionally to emphasize eventual effects of cortical feedback

Concluding the announcement of kernels and parameters is a remark of kernel  $K_{cr,s}$ . The cortical loop is already accounted for by the kernel  $K_{rcr,cen}$  and  $K_{exci,inhi}$ . As seen in the box below,  $K_{rcr,cen}$  and  $K_{exci,inhi}$  are assigned the connection from the cortical cells to the relay cell. The `connect()` method that makes the connection from the relay cell to the excitatory and inhibitory cortical cells need an argument that does not interfere with the loop kernel. The solution is to choose a  $\delta$ -function from equation ?? for the spatial and temporal part of the kernel. This is a natural solution because the Fourier-transformed of a  $\delta$ -function is one when  $t = 0$ , which is the default argument of the `create_delta_ft()` method.

```
# set impulse-response function
ganglion.set_kernel(kernel=(Wg_s, Wg_t))

# set coupling functions
network.connect(ganglion, relay, (Krg_s, Krg_t), 1.0)
network.connect(cortical_exci, relay,
                (Krcr_exci_s, Krcr_exci_t), 0.6)
network.connect(cortical_inhi, relay,
                (Krcr_inhi_s, Krcr_inhi_t), -0.6)
network.connect(relay, cortical_exci, (Kcr_s, Kcr_t), 1.0)
network.connect(relay, cortical_inhi, (Kcr_s, Kcr_t), 1.0)
```

**Listing 5.10:** Python code for establishing the connections between the neurons in the main network with pylgn

A final remark of the created network: In the kernel weight, as seen in the box above, are all set to one, except for the loop kernel, which is set to positive and negative 0.6. This parameter is chosen on the suggestion of Mobarhan. The cortical feedback might be "turn off" by setting the weight parameters for the cortical loop to zero. The polarity (ON or OFF) of the receptive field regions might be inverted by changing the signs of the weight parameters for the excitatory cell and the inhibitory cell. Note that they should always be opposite.

### 5.2.5 Stimuli

The stimuli often used to provoke neural response in visual experiments has been either moving bars (gratings), a patch with dynamic or static grating, or a simple flashing spot. Pylgn implements two different stimuli: "full-field grating" and "patch grating". The stimuli integrated in pylgn are given by a mathematical functions dependent of the wave number (spatial frequency),  $k_{pg}$ , the angular frequency,  $\omega_{pg}$ , the orientation,  $\theta$ , the contrast  $C$ , and the patch diameter,  $d$ . This is seen by the arguments of the `stimulus.create_fullfield_grating_ft()` method in the example application in section 5.2.1. The function for a patch grating is given by

$$s_{pg}(\vec{r}, t) = C(1 - \Theta(\vec{r} - d/2))\cos(\mathbf{k}_{pg}\vec{r} - \omega_{pg}t), \quad (5.1)$$

where  $\Theta(x)$  is the Heaviside step function. A static spot is obtained by setting  $k = \omega = 0$ . These are the two stimuli used for studying the effect of cortical feedback in this thesis. An oscillating spot is created by setting the spatial frequency,  $k_{pg}$ , of the stimulus equal to zero.



## Chapter 6

# Spatial Effects of Cortical Feedback on LGN Relay Cells,

It is desirable to compare the result provided by a model with the results from corresponding experimental data, to verify that the model account for the same qualitative tendencies as data. Experiments that remove cortical feedback (e.g. by surgical or pharmacological means) are scarce in literature [6]. However, Sillito et al [17] measured the effect of cortical feedback on the response properties of LGN relay cells. One of their experiments involved comparing responses of LGN cells to flashing circular spots to circular patches of drifting gratings. The experiment revealed that cortical feedback causes enhancement in the strength of patch suppression. Patch suppression is the reduction of the response to a large spot, compared to the maximum response to a spot covering just the receptive field center. This is illustrated in figure 6.1.

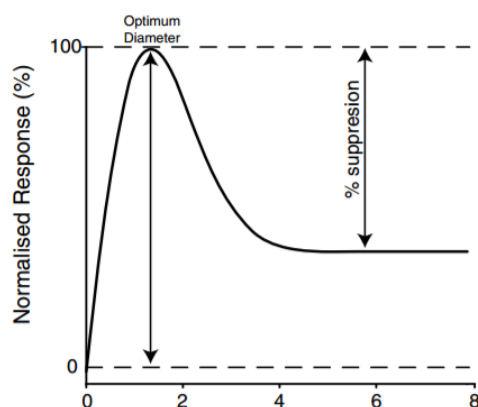


**Figure 6.1:** Illustration of patch suppression in a plot of response (y-axis) to stimuli with increasing patch diameter (x-axis). (From Sillito et al. [1])

## 36. SPATIAL EFFECTS OF CORTICAL FEEDBACK ON LGN RELAY CELLS,

The result of the experiment by Sillito et al. is summarised in figure 6.2. The figure shows that for circular spots the patch suppression is qualitatively the same with and without cortical feedback. For circular patches of drifting grating the experiment revealed a similar suppression when the feedback was intact, while the suppression was significantly reduced in the absence of cortical feedback.

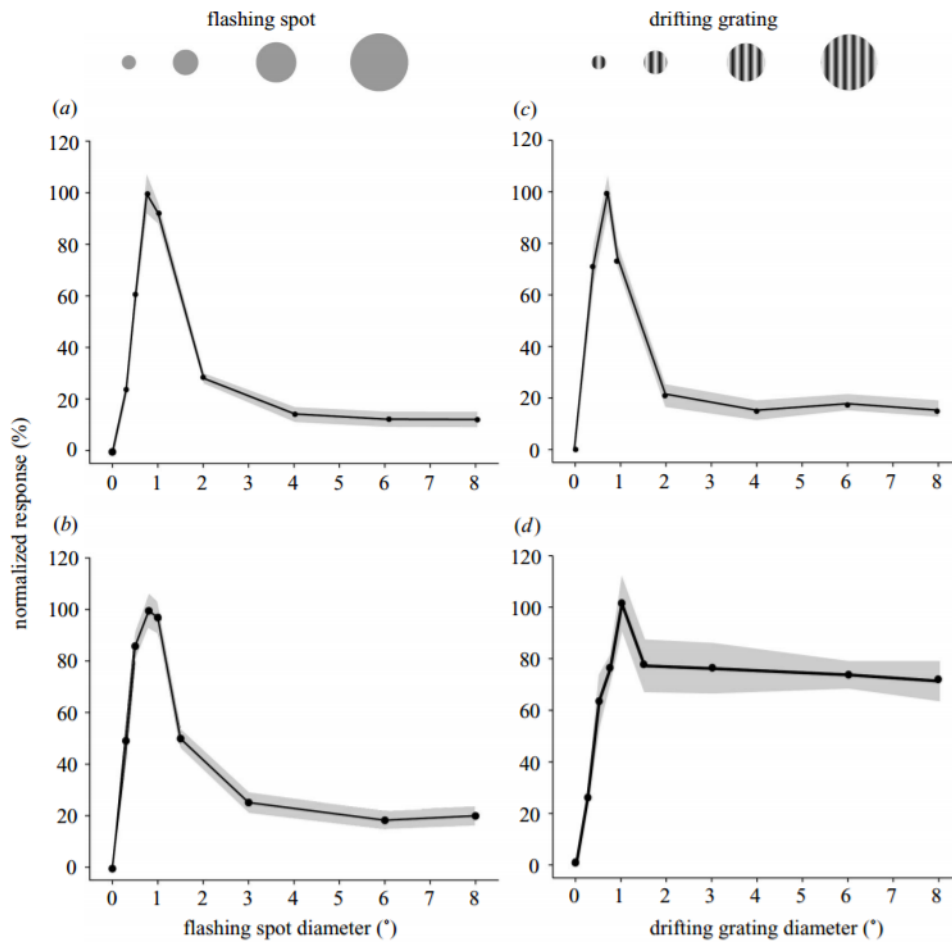


**Figure 6.2:** Effect of cortical feedback in LGN cells for varying diameter of stimulus. Plot a and b show responses to a flashing spot. Plot c and d show responses to patch grating. Plot a and c are from neurons with intact cortical feedback. Plot b and d show response of cells in the absence of feedback. (From Sillito et al. [17])

## 6.1 Previous Work Including eDoG Model and Pylgn

Mobarhan has used the experimental result provided by Sillito et al. [17] to explore feedback and feedforward parameter for the eDoG model with pylgn. Mobarhan plotted the center excitation and the surround inhibition for different widths of the center ( $a_{rcr}$ ) and surround ( $b_{rcr}$ ) excitation or inhibition, respectively. Figure 6.3 shows a difference-of-Gaussian function where "center excitation", and "surround inhibition" are indicated. Figure 6.3 illustrate that the terms "center excitation" and "surround inhibition" refers to the impulse-response function's max value of excitation and max value of inhibition, respectively. Figure 6.4 shows two plots from Mobarhans work [15]. The figures illustrate center excitation (left) and surround inhibition (right).

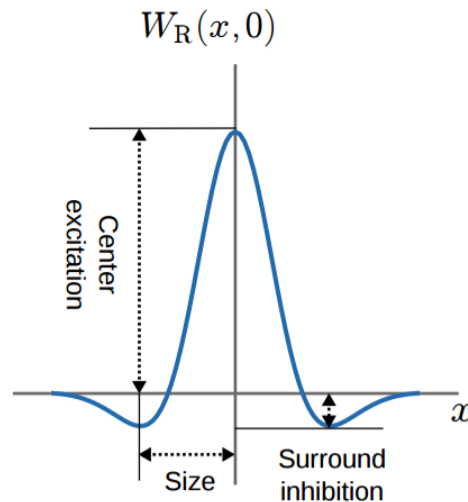


**Figure 6.3:** 2D plot of the spatial impulse-response function,  $W_r(x, y)$ , for the LGN relay cell modelled as a DoG function of the form in equation 3.1. The plot illustrates that the "center excitation" is the maximum value of excitation, and that the "surround inhibition" is the maximum value of inhibition. (From Mobarhan et al. [15])

From the experimental results of Sillito et al. it is established that feedback increase suppression of response to a patch stimuli with a certain size. Thus, the tendencies of interest is an increased excitation and inhibition. The sizes of the excitatory and inhibitory receptive field areas providing results in correspondence with these tendencies are chosen as Gaussian parameters for the mathematical model. Figure 6.4 is taken from Mobarhan's work [15]. The plots show that the suppression is greatest for small excitatory center widths and larger inhibitory surround widths.

This is the reason for the Gauss parameters  $a = 0.1$  and  $a = 0.9$  for the excitatory and inhibitory spatial feedback kernels,  $k_{\text{rcr,ex}}$  and  $k_{\text{rcr,in}}$ , respectively, which are described in section 5.

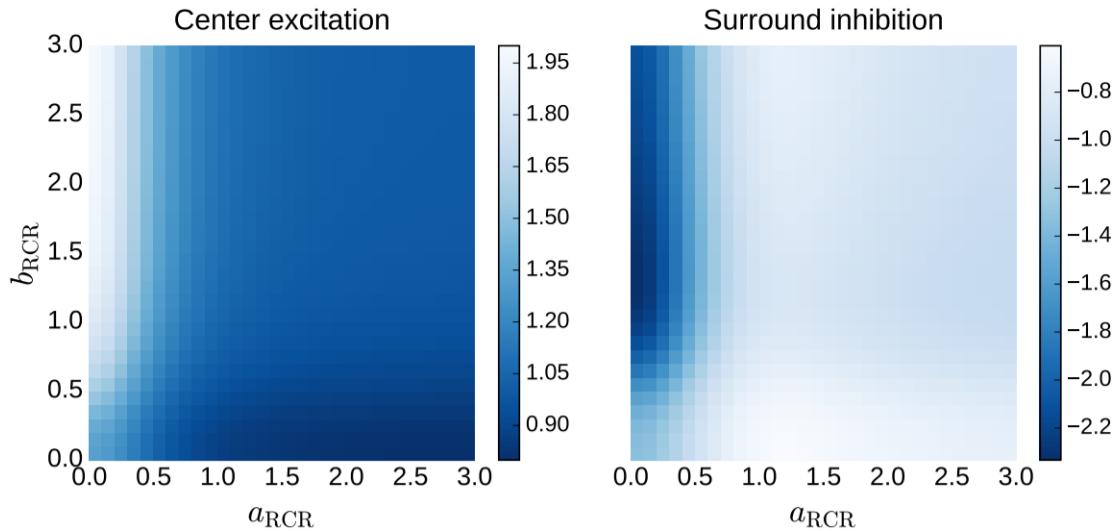


**Figure 6.4:** Plot of center excitation (left) and surround inhibition (right) for different widths of the center ( $a_{\text{rcr}}$ ) and surround ( $b_{\text{rcr}}$ ) receptive fields. (From Mobarhan et al. [15]).

This is just an example of parameter exploration by plotting and comparing to experimental characteristics. More exploration have been done for the feedback,  $k_{\text{fb}}$ , and the feedforward,  $k_{\text{ff}}$ , coupling kernels [?].

## 6.2 Validation of Network

All though the intentions with the plots in section 6.1 is to tune parameters, the plots will function as validation in this thesis. A method for validating the constructed network presented in chapter 5, is to recreate previous work. If the created network produces the same tendencies with the center excitation and surround inhibition as Mobarhan's results in figure 6.4, it can be concluded that the constructed network is reliable. Figure 6.5 shows a corresponding plot that shows center excitation and surround inhibition for the constructed network.

The plot in figure 6.5 shows the same tendencies as the previous work of Mobarhan in figure 6.3, thus the constructed network from chapter 5 is validated. The programme code used to create figure 6.5 is included in appendix B.



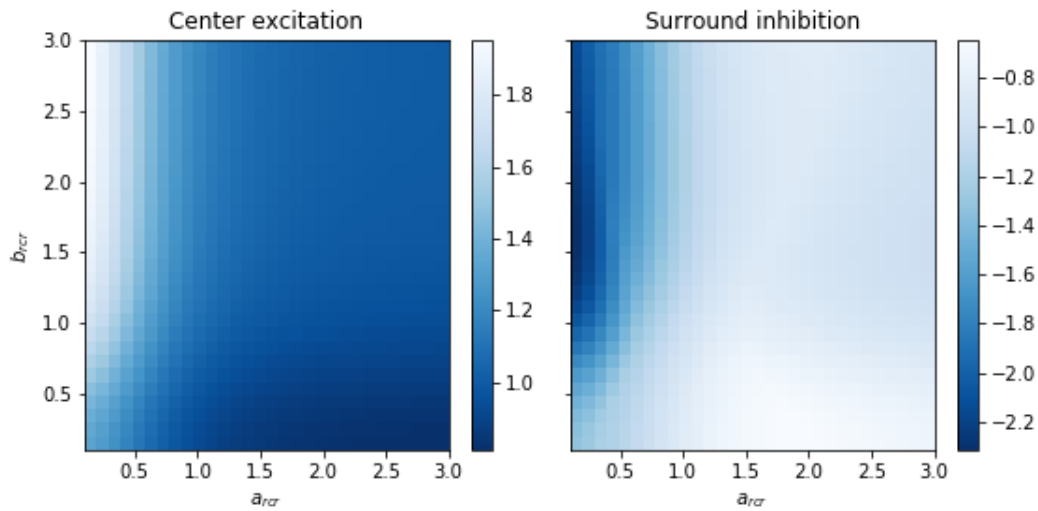


**Figure 6.5:** Plot of center excitation (left) and surround inhibition (right) from the impulse-response function for an LGN relay cell, according to the definition illustrated in figure 6.3. The simulation was performed with integrator parameters:  $nt = 1$ ,  $nr = 7$ ,  $dt = 1$  ms,  $dr = 1$  deg. The temporal kernels were modelled as Dirac  $\delta$ -functions. DoG parameters for the impulse response of ganglion cell,  $W_{g,s}$ :  $A = 1$ ,  $a = 0.62$ .deg,  $B = 0.85$ ,  $b = 1.26$ . Gauss parameters for the coupling kernel  $k_{rg,s}$ :  $A = 1$ ,  $a = 0.1$ . The excitatory and inhibitory cell's Gauss parameters:  $A = 1$  and  $A = 0.5$ , respectively, while  $a$  for both cells were varied between zero and three degrees. Feedback weight:  $w_{fb,ex} = 0,5$  and  $w_{fb,in} = -0,5$ . The remaining kernel weights were set to one. (Plot was generated in Spyder).

46. SPATIAL EFFECTS OF CORTICAL FEEDBACK ON LGN RELAY CELLS,

# Chapter 7

## Temporal Effects of Cortical Feedback on LGN Relay Cells

Section 5.2.4 explained that the temporal kernel for the feedback loop were chosen to be the exponential decay function in equation 3.4. The parameters of equation 3.4 are the delay  $\Delta$ , and time constant,  $\tau$ . These parameters represent the temporal features of cortical feedback in the constructed network. The time constant represent the ratio of decay of function 3.4, i.e. it determines for how long the feedback is effective on the response of the post-synaptic neuron. An increase in  $\tau_{fb}$  for cortical feedback is referred to as having a prolonged feedback. Another effect of increasing  $\tau_{fb}$  is a smaller maximum value of the temporal feedback kernel, as equation 3.4 in normalised with respect to  $\tau_{fb}$  itself. A relay cell's delay value represent the duration of the feedback loop, i.e. the delay between the signal transmttion from the reley cell and feedback received from cortex. As mentioned in section 2.2.4, the feedbackloop takes between three and ten ms. Thus, a delay value of 30 ms is an extreme value; an extreme value is chosen intentionally to emphasize possible influential effects. A time constant value of 1 is also an extreme value, chosen for the same purpose. A more reaonable value for the time constant of cortical feedback is 39 ms, accorting to Norheim et al. [16]. In this chapter feedback with delay value set to 30 ms (as opposed to 0 ms) are considered delayed, and feedback with time constant set to 39 ms (as opposed to 1 ms) are considered prolonged.

To explore how delay and prolonging of the feedback components affect the response of LGN relay cells, the response of an LGN relay cell were simulated for three different stimuli: An oscillating spot ( $k_{pg} = 0$  /deg), a patch grating with spatial frequency  $k_{pg} = 0,49$ /deg, and a patch grating with spatial frequency  $k_{pg} = 1,47$ /deg. Different combinations of values for the time constants,  $\tau$ , and the delay,  $\Delta$ , for the separate feedback components (excitatory and inhibitory) were explored in numerous simulations for each stimuli. First, two simulations were run where the feedback

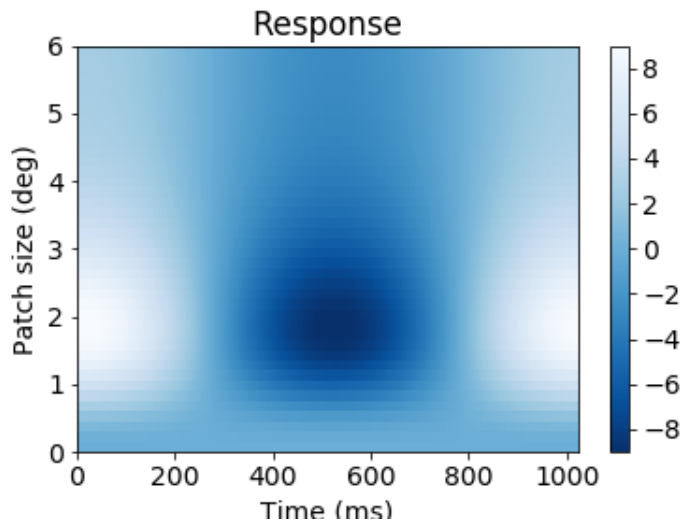
components were sequentially "turned off", by setting their feedback weight to zero. This served as another validation of the constructed network, as the outcome is foretold by definition, as explained in section 2.1.2. Secondly, simulations were done for networks with both excitatory and inhibitory feedback components included. Different combinations of delay and prolonging of the feedback components were implemented. For example, influence from a delayed excitatory feedback and a non-delayed inhibitory feedback, was explored by a simulation where the delay parameters were set accordingly:  $\Delta_{fb,ex} = 30\text{ms}$  and  $\Delta_{fb,in} = 0\text{ms}$ . The time constant was set to 1 ms for the exploration of effects provoked by delay. Then the same test was performed for both feedback components for delay, prolonging and a combination.

Neural response with respect to stimulus diameter and time are illustrated by colour maps, inspired by Einevoll et al. [4]. The plots show the spatiotemporal summation curve of LGN relay cell responses for stimulus diameters between zero and three degrees, during a time window from zero to 1023 ms. Each colour map presented in this chapter shows the result of a separate simulation of the constructed network described in chapter 5. The programme code that set up the network and simulates the LGN relay response to a visual stimuli and plots the summation curve is included in appendix A. Parameters that are not defined in the following sections have been set according to section 5.2.4 and appendix A.

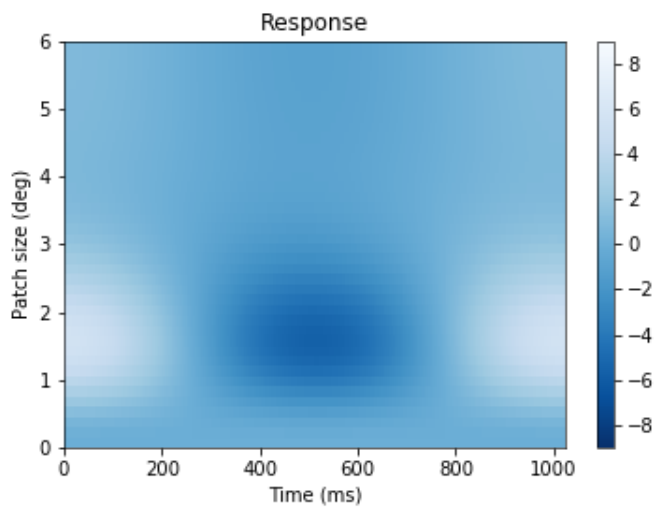
## 7.1 Response to Oscillating Spot

Figure 7.1 show the responses of an LGN relay cell when the network is stimulated with an oscillating spot with angular frequency  $\omega = 6, 14$  Hz, and cortical feedback are excluded. Figure 7.2 show the relay cell's response to the same stimulus when only inhibitory feedback is present. Figure 7.3 show the relay cell's response to the same stimulus when only the excitatory feedback is present. Figure 7.2 reveals reduction of neural response, and figure 7.3 reveals enhancement in neural response. These results agrees with theory, explained in chapter 2, and it is concluded that the simulations with pylgn provide the expected results.

Figure 7.4 show the response of an LGN relay cell for six different feedback scenarios for stimulus with an oscillating spot. All scenarios in figure 7.4 includes both excitatory and inhibitory feedback. In figure 7.4A and 7.4B delay was added to the excitatory and inhibitory feedback, respectively, excluding prolonging of feedback. In figure 7.4C and 7.4D prolonging was added to the excitatory and inhibitory feedback, respectively, excluding delay of feedback. In figure 7.4E and 7.4F delay was added to the excitatory and inhibitory feedback, respectively, while both feedback components were prolonged. As the spot oscillates, it has a push-pull effect (explained in section 3.1) on the LGN relay cell, and the cell's response is expected to oscillate with time (in the horizontal direction). The temporal oscillation is seen in



**Figure 7.1:** LGN relay cell response to an oscillating spot with angular frequency  $\omega = 6, 14$  Hz. No cortical feedback ( $w_{fb,ex,in} = 0$ ). (Figure generated in Spyder.)



**Figure 7.2:** LGN relay cell response to an oscillating spot with angular frequency  $\omega = 6, 14$  Hz, and removed excitatory feedback. The inhibitory feedback is delayed and prolonged. (Figure generated in Spyder.)

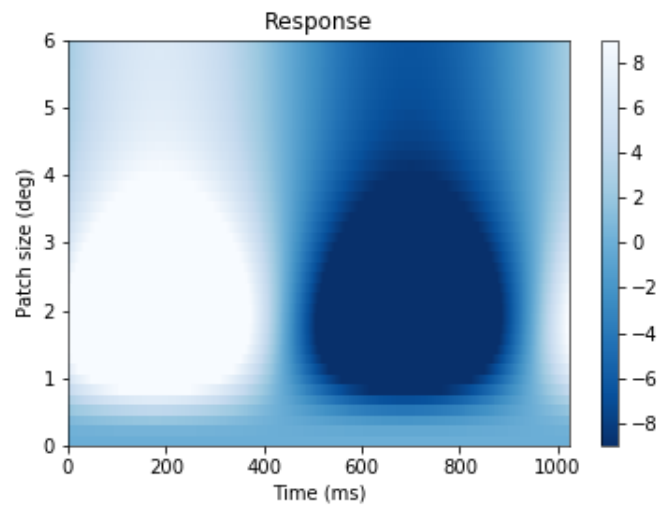


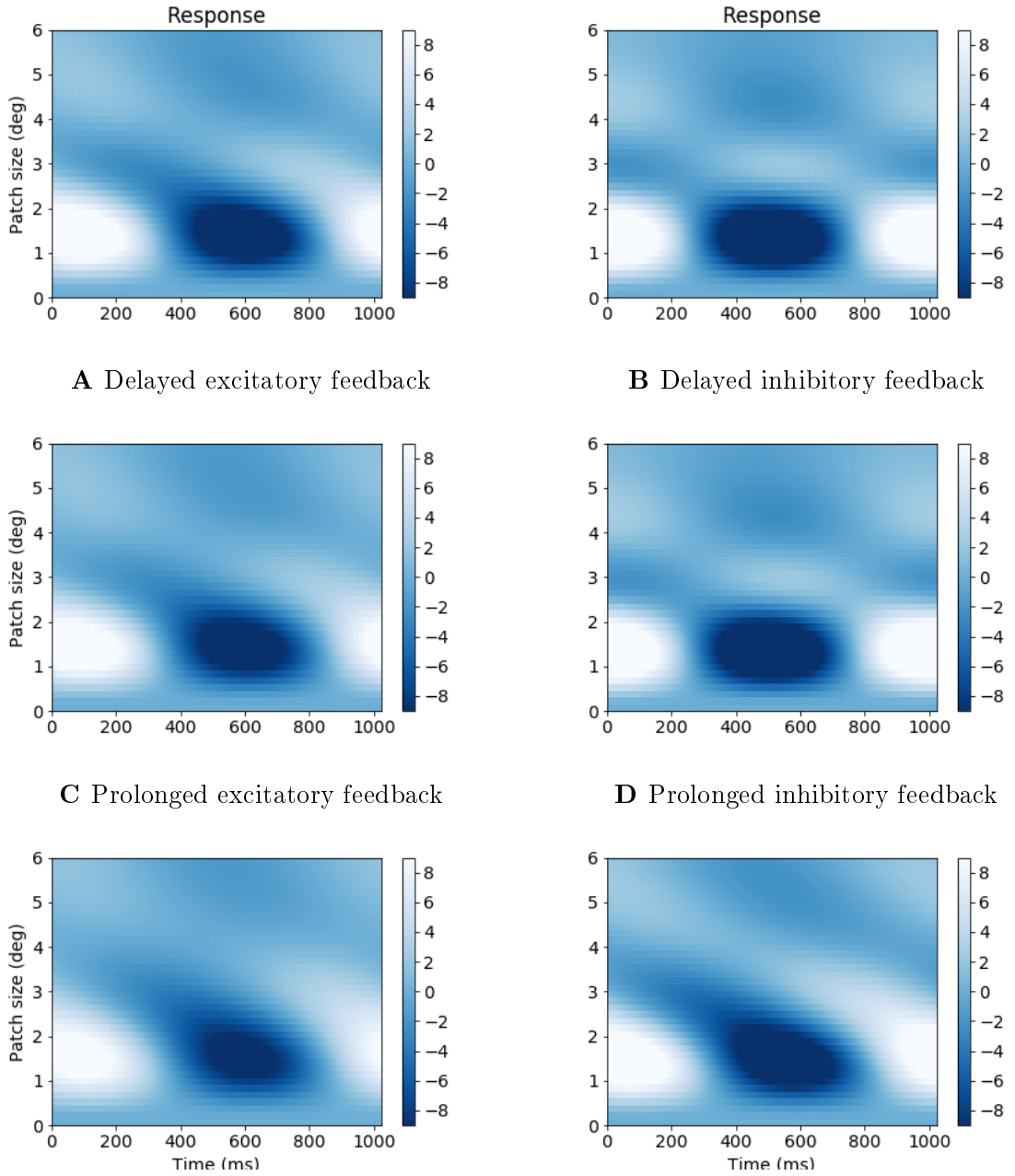
**Figure 7.3:** LGN relay cell response to an oscillating spot with angular frequency  $\omega = 6, 14$  Hz, and removed inhibitory feedback. The excitatory feedback is delayed and prolonged. (Figure generated in Spyder.)

all plots in figure 7.4, as expected. What is also seen in the plots is that the temporal oscillation varies with changes in spot size. In other words, the temporal oscillation of neural response is dependent of spot size. This non-linearity is apparent in all plots in figure 3.1). Although, the tendencies are weaker the feedback scenarios in figure 7.4B and 7.4D. These two figures both represent simulations where only the inhibitory feedback was either delayed or prolonged, while the excitatory feedback was neither. This result motivated to do an additional simulation, where the prolonging of the excitatory feedback was removed from the simulation that produced the plot in figure 7.4F. The result plot from the simulation is shown in figure 7.5. The new plot reveals a weaker dependence between the temporal oscillations and the spot size than the corresponding plot in figure 7.4F. This suggest that delay and prolonging of inhibitory feedback provoke neural response where the temporal oscillations are slightly less dependent of the spot size. It further indicates that delay and prolonging of the the excitatory feedback enhances dependency between oscillations and spot size. The response on the other hand seems to be reduced for the feedback scenarios where the excitatory component was prolonged figure 7.4C, 7.4E and 7.4F, compared to the remaining scenarios where the excitatory feedback was not prolonged.

The plots in figure 7.4 also indicate a relative tendency among themselves: the left column shows a general suppression of relay cell response compared to the right column. in other words, delay and prolonging of the excitatory feedback component reduces relay cell response compared to delay and prolonging of the inhibitory feed-

back component. It is evident that the inhibitory feedback is stronger compared to the excitatory feedback when the excitatory feedback is delayed or prolonged. The most relative suppression among the plots in figure 7.4 is seen for the scenarios where excitatory feedback are prolonged (7.4C, 7.4E and 7.4F). This suppression of neural response probably occur because of the normalisation of equation 3.4 by the time constant itself. In other words: Prolonged feedback have a lower response values for higher values of  $\tau$  with this choice of temporal feedback kernel.

Another evident divergence among the plots in figure 7.4F is that delay and/or prolonging of the excitatory feedback component (figures 7.4A, 7.4C and 7.4E) result in a temporal shift of the neural responses. The same tendency is not observed for delay and/or prolonging of inhibitory feedback in the remaining plots of figure 7.4.



**E** Delayed excitation. Prolonged excitatory and inhibitory feedback decay. **F** Delayed inhibition. Prolonged excitatory and inhibitory feedback decay.

**Figure 7.4:** Colour maps of LGN relay cell response to an oscillating spot with angular frequency  $\omega = 6, 14$  Hz and cortical feedback weight:  $w_{fb} = 0, 9$ . The plots show different scenarios for the cortical feedback. **A)** Delay:  $\Delta_{ex} = 30$  ms,  $\Delta_{in} = 0$  ms. Time constants:  $\tau_{ex,in} = 1$  ms. **B)** Delay:  $\Delta_{ex} = 0$  ms,  $\Delta_{in} = 30$  ms. Time constants:  $\tau_{ex,in} = 1$  ms. **C)** Delay:  $\Delta_{ex,in} = 0$  ms. Time constants:  $\tau_{ex} = 39$  ms,  $\tau_{in} = 1$  ms. **D)** Delay:  $\Delta_{ex,in} = 0$  ms. Time constants:  $\tau_{ex} = 1$  ms,  $\tau_{in} = 39$  ms. **E)** Delay:  $\Delta_{ex} = 30$  ms,  $\Delta_{in} = 0$  ms. Time constants:  $\tau_{ex,in} = 39$ ms. **F)** Delay:  $\Delta_{ex} = 0$  ms,  $\Delta_{in} = 30$  ms. Time constants:  $\tau_{ex,in} = 39$  ms. Other parameters were set according to section 5.2.4. (Plots generated in Spyder.)



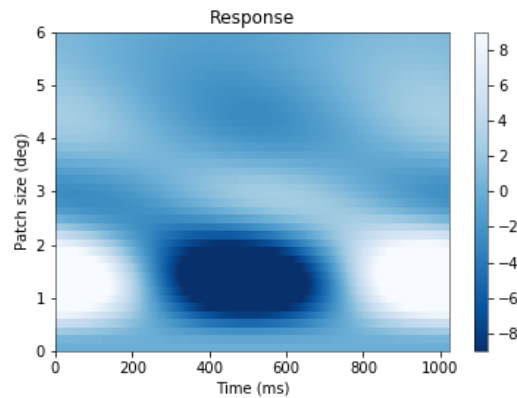


**Figure 7.5:** LGN relay cell response to an oscillating spot with angular frequency  $\omega = 6,14$  Hz. Cortical feedback weight:  $w_{fb} = 0,9$ . Feedback delay:  $\Delta_{ex} = 0$  ms,  $\Delta_{in} = 30$  ms. Feedback time constants:  $\tau_{ex} = 1$  ms,  $\tau_{in} = 1$  ms. (Figure generated in Spyder).

## 7.2 LGN Rerlay cell Response to Patch Grating

The same procedure as in section 7.1 was preformed for LGN relay cell response to a patch grating with angular frequency  $\omega = 6,14$ Hz and spatial frequency  $k = 0,49$ /deg. The neural response to this patch grating was identical as for the oscillating spot. For this reason the pots are not included in this thesis, and it was concluded that an angular frequency of  $0,49$ /deg in a patch grating is not great enough to provoke other responses than a simple spot.

Thereafter, the same procedure as in section 7.1 was preformed for relay cell response to a patch grating with higher angular frequency  $\omega = 6,14$ Hz, and spatial frequency  $k = 1,47$ /deg. Figure 7.6 show the response of an LGN relay cell without cortical feedback. Figure 7.7 show several simulations of the neural response where cortical feedback are included, for the same feedback scenarios as for an oscillating spot in the previous section. The plots in figure 7.7 show the same tendency of reduction in neural response as for an oscillating spot. In contrast to the response to an oscillating spot, the responses in figure 7.7 shows an approximately linear neural response to the stimulus of higher spatial frequency. This justifies an assumptions for linearity for response of LGN relay cells to stimulus of patch grating with greater spatial frequencies.

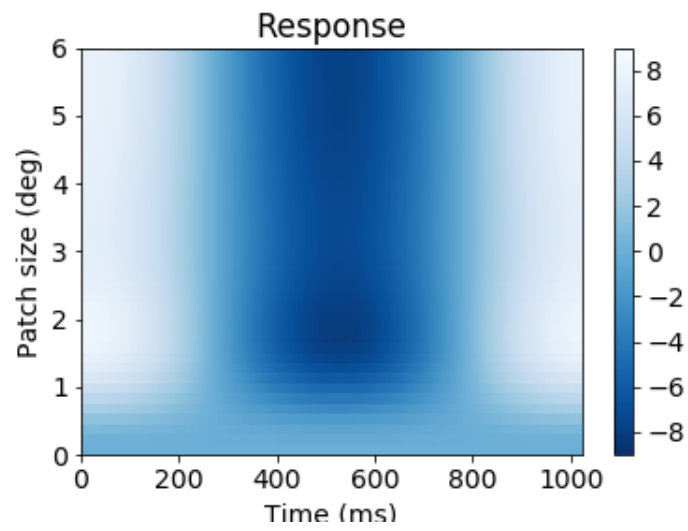
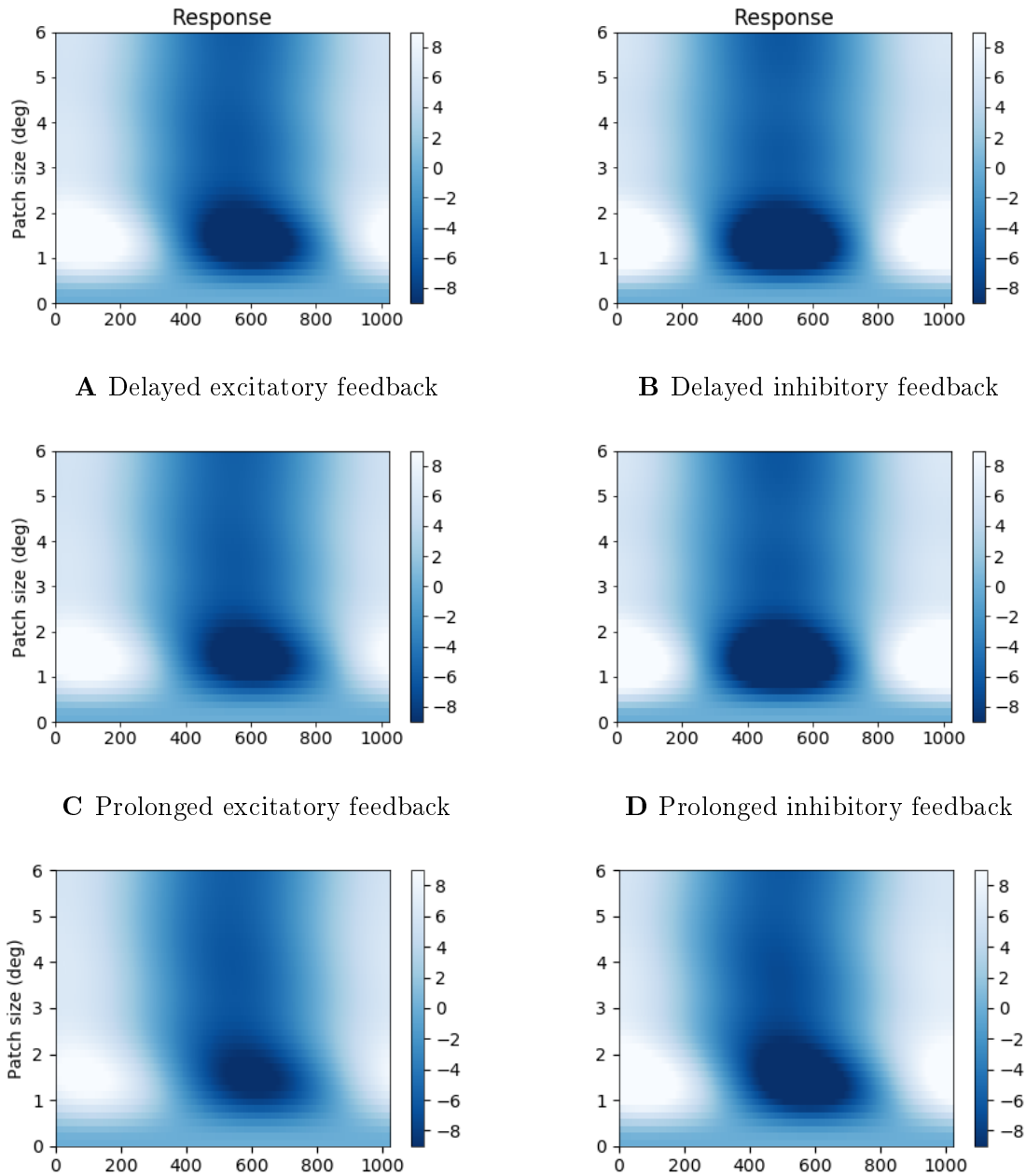


**Figure 7.6:** LGN relay cell response to a flashing spot with wave number  $\approx 1.47/\text{deg}$  and angular frequency  $\omega = 6, 14$  Hz. (Figure generated in Spyder.)



**E** Delayed excitation. Prolonged excitatory and inhibitory feedback decay. **F** Delayed inhibition. Prolonged excitatory and inhibitory feedback decay.

**Figure 7.7:** Colour maps of LGN relay cell response to a flashing spot wave number  $\omega = 1.47/\text{deg}$  and angular frequency  $\omega = 6, 14$  Hz. Cortical feedback weight  $w_{fb} = 0, 9$ .  
**A)** Feedback delay:  $\Delta_{ex} = 30$  ms,  $\Delta_{in} = 0$  ms. Feedback time constants:  $\tau_{ex,in} = 1$  ms.  
**B)** Feedback delay:  $\Delta_{ex} = 0$  ms,  $\Delta_{in} = 30$  ms. Feedback time constants:  $\tau_{ex,in} = 1$  ms.  
**C)** Feedback delay:  $\Delta_{ex,in} = 0$  ms. Feedback time constants:  $\tau_{ex} = 39$  ms,  $\tau_{in} = 1$  ms.  
**D)** Feedback delay:  $\Delta_{ex,in} = 0$  ms. Feedback time constants:  $\tau_{ex} = 1$  ms,  $\tau_{in} = 39$  ms.  
**E)** Feedback delay:  $\Delta_{ex} = 30$  ms,  $\Delta_{in} = 0$  ms. Feedback time constants:  $\tau_{ex,in} = 39$ ms.  
**F)** Feedback delay:  $\Delta_{ex} = 0$  ms,  $\Delta_{in} = 30$  ms. Feedback time constants:  $\tau_{ex,in} = 39$  ms.  
 Other parameters were set according to section 5.2.4. (Plots generated in Spyder.)

### 7.3 Significance of Results

The response of an LGN relay cell to an oscillating spot shows a non-linear effect; the temporal oscillation of neural response is dependent of spot size. This is an interesting feature, but it is not due to delay or prolonging of feedback components. One could argue that the result is relevant for the research question, because the dependence was strengthened when the excitatory feedback component was delayed or had a higher time constant compared to the inhibitory feedback component. Though, this is only a feature of the relationship between the excitatory and inhibitory feedback. Otherwise, the only evident effect of delay and prolonging of the separate feedback components was due to the normalisation of the temporal feedback kernel. So to answer the research question: The effect of delay and prolonging of separate feedback components is none other than the intrinsic values of excitatory and inhibitory feedback. Obviously another research question should have been asked for this thesis. Changes of delay and the time constant only reveal tendencies of in excitatory and inhibitory feedback relative to each other, which is already known. For example, when prolonging the excitatory feedback component it is also reduced in value, and the inhibition from the cortical feedback will have a greater effect. If anything, the results of the simulations in this thesis demonstrated the uselessness of comparing the time constant to the delay.

The potential in such an efficient mathematical model designed to explore the effects of cortical feedback, incorporated into a relative intuitive and applicable simulation tool, should have been used in a more constructive way than demonstrated in this thesis. At least the second objective of this thesis can be answered more constructively. The simulations of responses of LGN relay cells performed with `pylgn` have shown results in accordance with general accepted theory. For example, suppression of LGN cell response when stimulus sizes are magnified over a certain diameter value. The application of the circuit simulation software is intuitive from a programming perspective. The only downside have been the need for guiding in the choice of grid parameters compared to the kernel parameters. Consideration of grid parameters compared to kernel parameter is necessary due to the transformation of kernels into Fourier space, as this demands that the kernels converge to zero within the defined grid. This makes the simulation software less intuitive for the general user. Nevertheless, `pylgn` provides a great range of opportunities for research of neural responses to stimuli.

The network constructed with `pylgn` for this thesis, which separated the excitatory and inhibitory feedback components could come in handy if applied on a better manner. A better manner would be to explore temporal aspects of delay alone, and keep the time constant as a constant. Another idea is to explore the temporal aspect of cortical feedback with a non-linear mathematical model. Although, the

---

non-linearities evident in these simulations are minimal compared to the general neural response, so a simplified, linear mathematical model like the eDoG model should be sufficient for future exploration of this kind. Another idea for future work is the exploration of non-separable time kernels, which is a possibility with pylgn. All in all, pylgn has a lot of potential, though used to study wrong temporal aspects in this thesis.



# Bibliography

- [1] Ian M. Andolina, Helen E. Jones, and Adam M. Sillito. Effects of cortical feedback on the spatial properties of relay cells in the lateral geniculate nucleus. *Journal of Neurophysiology*, 109(3):889–899, 2013.
- [2] Peter Dayan and I. F. Abbott. *Theoretical Neuroscience - Computational and Mathematical Modelling of Neural Systems*. The MIT Press, Cambridge, 2005.
- [3] Gaute T. Einevoll and Geir Halnes. Lateral geniculate nucleus (lgn) models. pages 1490–1495, 2014.
- [4] Gaute T. Einevoll, Paulius Jurkus, and Paul Heggelund. Coarse-to-fine changes of receptive fields in lateral geniculate nucleus have a transient and a sustained component that depend on distinct mechanisms. *PLOS ONE*, 6(9):1–19, 09 2011.
- [5] Gaute T. Einevoll and Hans E. Plesser. Linear mechanistic models for the dorsal lateral geniculate nucleus of cat probed using drifting grating stimuli. 13(4):503–530, 2002.
- [6] Gaute T. Einevoll and Hans E. Plesser. Extended difference-of-Gaussian model incorporating cortical feedback for relay cells in the lateral geniculate nucleus of cat. 6(4):307–324, 2012.
- [7] Ralph D. Freeman Gregory C. DeAngelis, Izumi Ohazawa. Receptive-field dynamics in the central visual pathway. *Trends in Neuroscience*, 18(10):451–458, 1995.
- [8] Judith A. Hirsch, Xin Wang, Friedrich T. Sommer, and Luis M. Martinez. How inhibitory circuits in the thalamus serve vision. *Annual Review of Neuroscience*, 38(1):309–329, 2015.
- [9] Milad Hobbi Mobarhan. A firing-rate based simulation tool for studying roles of cortical feedback in lateral geniculate nucleus (lgn). '<http://miladh.github.io/lgn-simulator/doc/about.html>', 2016. Accessed: 2017-05-02.

- 
- [10] Milad Hobbi Mobarhan. A firing-rate based simulation tool for studying roles of cortical feedback in lateral geniculate nucleus (lgn). '<http://pylgn.readthedocs.io/en/latest/index.html>', 2017. Accessed: 2017-01-05.
- [11] Milad Hobbi Mobarhan. Simulator for the early visual system. '<https://github.com/miladh/pylgn/>', 2017. Accessed: 2017-05-01.
- [12] Luis M. Martinez, Manuel Molano-Mazón, Xin Wang, Friedrich T. Sommer, and Judith A. Hirsch. Statistical wiring of thalamic receptive fields optimizes spatial sampling of the retinal image. *Neuron*, 81(4):943–956, 2014.
- [13] Luke Mastin. Neurons and synapses. '[http://www.human-memory.net/brain\\_neurons.html](http://www.human-memory.net/brain_neurons.html)', 2010. Accessed: 2017-02-31.
- [14] Helene B. Midtjord. Application of the lgn simulator. '<https://github.com/helenebm/pylgn-project/>', 2017. Accessed: 2017-01-05.
- [15] Milad H. Mobarhan, Geir Halmes, Pablo Martínez-Cañada, Torkel Hafting, Marianne Fyhn, and Gaute T. Einevoll. A Firing-rate Based Simulation Tool for Studying Roles of Cortical Feedback in Lateral Geniculate Nucleus. Centre for Integrative Neuroplasticity, 2017.
- [16] E. S. Nordheim, J. Wyller, E. Nordlie, and G. T. Einevoll. A minimal mechanistic model for temporal signal processing in the lateral geniculate nucleus. *Cognitive Neurodynamics*, 6(4):307–324, 2012.
- [17] Adam M. Sillito and Helen E. Jones. Corticothalamic interactions in the transfer of visual information. *Philosophical Transactions of the Royal Society of London B: Biological Sciences*, 357(1428):1739–1752, 2002.



# Appendix A

## Programme Code for Simulation of Response in LGN Relay Cell to Different Stimuli with Pylgn

```
# -*- coding: utf-8 -*-

import quantities as pq
import numpy as np
import matplotlib.pyplot as plt
import os

import pylgn
import pylgn.kernels.spatial as spl
import pylgn.kernels.temporal as tpl

# variables
w_fb = 0.9          # 0 -> no feedback.
k_pg_index = 3     # 0-> k=0. 1-> k=0.49. 3-> k=1.47.
exDelay = 5
inDelay = 20
exTau = 39
inTau = 39

# diameters
mask_size = np.linspace(0, 6, 40)*pq.deg

# list to store spatiotemporal summation curves for each
weight
responses = []
```

```

# create network
network = pylgn.Network()

# create integrator
integrator = network.create_integrator(nt=10, nr=7, dt=1*pq.ms
    , dr=0.1*pq.deg)

# create spatial kernels
Wg_s = spl.create_dog_ft(A=1, a=0.62*pq.deg, B=0.85, b=1.26*pq
    .deg)
Krg_s = spl.create_gauss_ft(A=1, a=0.1*pq.deg)
Kcr_s = spl.create_delta_ft()
Krcr_exci_s = spl.create_gauss_ft(A=1, a=(0.1)*pq.deg)
Krcr_inhi_s = spl.create_gauss_ft(A=2, a=(0.9)*pq.deg)

# create temporal kernels
Wg_t = tpl.create_biphasic_ft(phase_duration =42.5*pq.ms,
    damping_factor =0.38, delay =0 *
    pq.ms)
Krg_t = tpl.create_exp_decay_ft(18*pq.ms, delay = 0 *pq.ms)
Kcr_t = tpl.create_delta_ft()
Krcr_exci_t = tpl.create_exp_decay_ft(exTau*pq.ms, delay =
    exDelay*pq.ms)
Krcr_inhi_t = tpl.create_exp_decay_ft(inTau*pq.ms, delay =
    inDelay*pq.ms)

# create neurons
ganglion = network.create_ganglion_cell(kernel=(Wg_s, Wg_t))
relay = network.create_relay_cell()
cortical_exci = network.create_cortical_cell()
cortical_inhi = network.create_cortical_cell()

# connect neurons
network.connect(ganglion, relay, (Krg_s, Krg_t), 1.0)
network.connect(cortical_exci, relay, (Krcr_exci_s,
    Krcr_exci_t), w_fb)
network.connect(cortical_inhi, relay, (Krcr_inhi_s,
    Krcr_inhi_t), -w_fb)
network.connect(relay, cortical_exci, (Kcr_s, Kcr_t), 1.0)
network.connect(relay, cortical_inhi, (Kcr_s, Kcr_t), 1.0)
    
```

```

st_summation_curve = np.zeros([len(mask_size), integrator.Nt])
    / pq.s
for i, d in enumerate(mask_size):
    # create stimulus
    k_pg = integrator.spatial_freqs[k_pg_index]
    w_pg = integrator.temporal_freqs[1] #=6.14 Hz. Set to 0
    for static stimuli
        stimulus = pylgn.stimulus.create_patch_grating_ft(
            wavenumber=k_pg,

            angular_freq=w_pg,

            mask_size=d)
        network.set_stimulus(stimulus)

        # compute
        network.compute_response(relay, recompute_ft=True)
        st_summation_curve[i, :] = relay.center_response
    responses.append(st_summation_curve)

# save fig
if k_pg_index == 0:
    form = 'FS'
else:
    form = 'PG'

if w_fb == 0:
    feedback = 'NoFB'
else:
    feedback = 'FB'

my_path = '□' # insert path
my_file = '{}_k{}_{}_exDelta{}_inDelta{}_exTau{}_inTau{}.png'.
    format(feedback,
           k_pg_index, form, exDelay, inDelay, exTau, inTau)

# clear network
network.clear()

# xmin, xmax, ymin, ymax:
extent = [integrator.times.min(), integrator.times.max(),
          mask_size.min(), mask_size.max()]

```

```
vmin = -9
vmax = 9

# visualize
plt.imshow(responses[0], extent=extent, origin="lower", aspect
           ="auto",
           vmin=vmin, vmax=vmax, cmap='Blues_r', )

plt.title("Response")
plt.ylabel("Patch_size(deg)")
plt.xlabel("Time(ms)")

plt.colorbar(aspect=23)
plt.savefig(os.path.join(my_path, my_file), format='png')
plt.show()
```

**Listing A.1:** Plotting Spatiotemporal Summation Curve for Different Stimuli

## Appendix B

# Plotting Impulse-Response for Spatial Parameters

```
import quantities as pq
import numpy as np
import matplotlib.pyplot as plt

import pylgn
import pylgn.kernels.spatial as spl
import pylgn.kernels.temporal as tpl

center_excit_norm = 0.397736473073
surround_inhib_norm = 0.0302344189143

a_rcr_vec = np.linspace(0.1, 3.0, 30) * pq.deg
b_rcr_vec = np.linspace(0.1, 3.0, 30) * pq.deg

center_excit = np.zeros([len(b_rcr_vec), len(a_rcr_vec)])
surround_inhib = np.zeros([len(b_rcr_vec), len(a_rcr_vec)])

for i, b_rc in enumerate(b_rcr_vec):
    for j, a_rc in enumerate(a_rcr_vec):
        network = pylgn.Network()

        # create integrator
        integrator = network.create_integrator(nt=1, nr=7, dt
=1*pq.ms, dr=1*pq.deg)

        # create spatial kernels
```

```

    Wg_s = spl.create_dog_ft(A=1, a=0.62*pq.deg, B=0.85, b
=1.26*pq.deg)
    Krg_s = spl.create_gauss_ft(A=1, a=0.1*pq.deg)
    Kcr_s = spl.create_delta_ft()
    Krcr_cen_s = spl.create_gauss_ft(A=1, a=(a_rc))
    Krcr_sur_s = spl.create_gauss_ft(A=0.5, a=(b_rc))

    # create temporal kernel
    delta_t = tpl.create_delta_ft()

    # create neurons
    ganglion = network.create_ganglion_cell(kernel=(Wg_s,
delta_t))
    relay = network.create_relay_cell()
    cortical_cen = network.create_cortical_cell()
    cortical_sur = network.create_cortical_cell()

    # connect neurons
    network.connect(ganglion, relay, (Krg_s, delta_t),
1.0)
    network.connect(cortical_cen, relay, (Krcr_cen_s,
delta_t), 0.5)
    network.connect(cortical_sur, relay, (Krcr_sur_s,
delta_t), -0.5)
    network.connect(relay, cortical_cen, (Kcr_s, delta_t),
1.0)
    network.connect(relay, cortical_sur, (Kcr_s, delta_t),
1.0)

    network.compute_irf(relay)

    center_excit[i, j] = np.real(relay.irf[0].max()) /
center_excit_norm
    surround_inhib[i, j] = np.real(relay.irf[0].min()) /
surround_inhib_norm

# visualize
fig, (ax1, ax2) = plt.subplots(nrows=1, ncols=2, figsize=(8,
4), sharey="row")

# xmin, xmax, ymin, ymax:

```

```
extent = [a_rcr_vec.min(), a_rcr_vec.max(), b_rcr_vec.min(),
          b_rcr_vec.max()]

im1 = ax1.imshow(center_excit, extent=extent, origin="lower",
                 aspect="auto", cmap="Blues_r")
ax1.set_title("Center_□excitation")
ax1.set_ylabel("$b_{rcr}$")
ax1.set_xlabel("$a_{rcr}$")
plt.colorbar(im1, ax=ax1)

im2 = ax2.imshow(surround_inhib, extent=extent, origin="lower"
                 , aspect="auto", cmap="Blues_r")
ax2.set_title("Surround_□inhibition")
ax2.set_xlabel("$a_{rcr}$")
plt.colorbar(im2, ax=ax2)
plt.tight_layout()
plt.show()
```

**Listing B.1:** Plotting Impulse response for Spatial Parametersæ











Norges miljø- og biovitenskapelig universitet  
Noregs miljø- og biovitenskapelige universitet  
Norwegian University of Life Sciences

Postboks 5003  
NO-1432 Ås  
Norway